이학박사 학위논문

중증열성혈소판감소증후군 바이러스 중화 항체의 개발과 검증에 대한 연구

Development and evaluation of neutralizing antibody against Severe Fever with Thrombocytopenia Syndrome Virus

2019 년 8 월

서울대학교 대학원

협동과정 종양생물학 전공

김 기 현

Abstract

Development and evaluation of neutralizing antibody against Severe Fever with Thrombocytopenia Syndrome Virus

Ki Hyun Kim

Cancer Biology Major

Graduate School of Seoul National University College of Medicine

Severe fever with thrombocytopenia syndrome (SFTS) is an emerging infectious disease localized to China, Japan, and Korea that is characterized by severe hemorrhage and a high fatality rate. Currently, no specific vaccine or treatment has been approved for this viral disease. To develop a therapeutic agent for SFTS, we isolated antibodies from a phage-displayed antibody library that was constructed from a patient who recovered from SFTS virus (SFTSV) infection. One antibody, designated as Ab10, was reactive to the Gn envelope glycoprotein of

SFTSV and protected host cells and A129 mice from infection in both in vitro and in vivo experiments. Notably, Ab10 protected 80% of mice, even when injected 5 days after inoculation with a lethal dose of SFTSV. Using cross-linker assisted mass spectrometry and alanine scanning, we located the non-linear epitope of Ab10 on the Gn glycoprotein domain II and an unstructured stem region, suggesting that Ab10 may inhibit a conformational alteration that is critical for cell membrane fusion between the virus and host cell. Ab10 reacted to recombinant Gn glycoprotein in Gangwon/Korea/2012, HB29, and SD4 strains. Additionally, based on its epitope, we predict that Ab10 binds the Gn glycoprotein in 247 of 272 SFTSV isolates previously reported. Together, these data suggest that Ab10 has potential to be developed into a therapeutic agent that could protect against more than 90% of reported SFTSV isolates.

Keywords: Emerging virus, Severe Fever with Thrombocytopenia Syndrome Virus, Virus neutralizing antibody, Monoclonal antibody therapeutics

Student number: 2015-30613

Table of contents

Table of figures

1 Introduction

1.1 Virologic characteristics of SFTSV

1.1.1 Classification

SFTSV, the emerging tick-borne virus was once classified as a member of the *Phlebovirus* genus, *Phenuiviridae* family, and *Bunyavirales* order until the major update of taxonomy related to numerous bunyaviruses and ratifications on October 2018 (Master Species List #33) [1] and on February 2019 (Master Species List #34) [2] by the International Committee on Taxonomy of Viruses (ICTV).

At present, SFTSV is classified as the newly assigned species called Huaiyangshan banyangvirus. This species group is the only species in the genus *Banyangvirus*, which is associated to the reestablished taxonomy of family *Phenuiviridae*, order *Bunyavirales*, class *Ellioviricetes*, phylum *Negarnaviricota*, realm *Riboviria*. Although ICTV currently accepts the changed name, the term SFTSV is much more widely used until now.

1.1.2 Genome

As a member of *Bunyavirales* order, which belongs to a class V virus group based on Baltimore classification, SFTSV is a single-stranded negative-sense tripartite RNA virus. The genome of SFTSV is comprised of a large (L) segment with 6,368 nucleotides, medium (M) segment with 3,378 nucleotides, and small (S) segment with 1,744 nucleotides. These tripartite genomes encode the RNA-dependent RNA polymerase (L segment), envelope Gn glycoprotein (M segment), envelope Gc glycoprotein (M segment), nucleoprotein (S segment), and nonstructural proteins (S segment)[3].

1.1.3 Genetic diversity

Lack of proofreading function in RNA-dependent RNA polymerase used for SFTSV replication provided a base for genetic diversity. A phylogenetic analysis based on genome sequences of SFTSV isolates found substantial genetic diversity and accumulated mutations, suggesting that SFTSV has existed for decades at minimum[4,5]. According to the phylogenetic analysis of three genomic segments from China, Japan, and South Korea, six genotypes (phylogenetic groups or sub-lineages) of SFTSV have been identified. Among six genotypes of A to F, All the

genotypes except B were discovered across six providences of China. In the other hand, in Japan, only genotype B was identified. In South Korea, genotypes B, D, and F were found. However, the difference in virulence between these SFTSV sub-lineages has yet to be determined and remains to be elucidated.

Moreover, due to geological feature of Huaiyangshan area where located in junctions of Anhui, Henan, Hubei providence of China, multiple SFTSV isolates with genetic reassortment among segments were also found along with pure genotypes. Except for Huaiyangshan area, six more genetic reassortment cases were identified in Anhui, Henan, Liaoning provinces[6]. Furthermore, the case of homologous recombination within M segment between two different sub-lineages of SFTSV was reported[7]. These findings indicate that genotypes of SFTSV have become diverse rapidly with a high mutation rate of RNA genome replication and suggest that more precise and structured genotype nomenclature is required for further research or international collaboration[8].

1.2 Epidemiological and ecological characteristics of SFTS

1.2.1 Incidence and case fatality rate

Since its isolation as a novel virus and the following report in 2011[9], cases of the acute infectious disease called SFTS have risen rapidly in China, Japan, and Korea, posing a risk to public health and increasing the fear of ticks that transmit the deadly SFTSV.

Although the first isolation of SFTSV was published in 2011, according to the retrospective study[10], SFTS cases were found since 2007 in Henan province. Serum samples of 238 patients with suspected infectious disease from 2007 to 2010 were tested positive for SFTSV infection by RT-PCR and indirect immunofluorescence assay. A number of cases found were 79 in 2007 with case fatality rate of 12.7%. Case fatality rate between 2008 and 2010 was not described.

From 2011 to 2016, SFTSV infected 5,360 people in China with an average case fatality rate of 6.40%[11]. After initial reports in 2013 of sporadic SFTS cases in South Korea[12] and Japan[13], South Korea reported

866 cases with an average case fatality of 20.0%[14] and Japan reported 388 cases with an average fatality of 15.7%[15] from 2013 to 2018.

Although the exact number of the SFTS cases in China is controversial among publications[5,11], the number of SFTS cases is undoubtedly increasing in China, and the number of laboratory-confirmed cases from 2011 to 2016 were 461, 579, 1034, 1304, and 1306. Notably, among 5,360 reported cases, the highest numbers of reported cases (2025 cases) were from Henan province, accounting for 37% of total in China. Considering the population of Henan province, which is 95.32 million in 2013, prevalence of SFTS in this particular province is much higher than South Korea. Excluding Henan province, most of the SFTS cases in China were limited to other 6 provinces. In the same period, 1,515 cases from Shandong province, 663 cases from Hubei province, 502 cases from Anhui province, 260 cases from Zhejiang province, 224 cases from Liaoning province, and 146 cases from Jiangsu province were reported[11].

In South Korea, cases of SFTS are increasing gradually from the year of first identification in 2013. The number of cases from 2013 to 2017 were 36, 55, 79, 165, and 272 respectively. Recently in 2018, mercifully, however, the number of SFTS cases and death cases was slightly

decreased compared to the previous year, counting for 259 SFTS cases with 46 death cases[14].

The overall mortality of SFTS patients ranged from 6% to 30% depending on area of incidence and also varied in studies[9,16–19]. Low case fatality rate in Henan province which constitutes the biggest portion of cases in China could have led to fluctuation of case fatality rates in various reports[18]. Otherwise, different sub-lineages of SFTSV in each region or countries were possibly destined to have variations in virulence and directed to the effect on case fatality rate consequently[20]. In the other hand, seasonal distributions of SFTS cases are apparent. Generally, the SFTS endemic occurs between March and November, and peaks around May[5].

1.2.2 Vectors

Viruses of *Phenuiviridae* family are vector-borne, mainly transmitted by arthropods such as ticks, fleas, mosquitos, or sandflies. Above all, ticks such as *Haemaphysalis longicornis* and *Rhipicephalus microplus* are implicated as the prominent vectors for transmitting SFTSV since SFTSV RNA was found in 4.93% of *H.longicornis* pools and in 0.61% of *R.microplus* pools collected in endemic regions of Hubei and Henan provinces[21]. Moreover, identification of SFTSV RNA positive

Amblyomma testudinarium, *Ixodes nipponensis* ticks collected from humans in South Korea suggested that various species of ticks could serve as potential SFTSV vectors[22]. Furthermore, the discovery of *H. longicornis* tick in the United States indicates the possibility that SFTSV could spread to other continents, highlighting the need to prevent disease transmission across the world[23].

1.2.3 Hosts

With regards to SFTSV hosts, various vertebrate species are considered to have been infected. Domestic animals are respected to be a critical reservoir hosts for SFTSV and ticks as evidenced by high SFTSV seroprevalence in various animals in SFTS endemic regions[24,25]. In the report, more than 80% of goats in the village in Shandong province were seropositive for SFTSV when measured by double-antigen sandwich ELISA[26]. Besides, in investigation of 3,039 domestic animals in two epidemic regions, 69.5% of sheep, 60.5% of cattle, 37.9% of dogs, 3.1% of pigs, 47.4% of chickens were found to have SFTSV specific antibodies[27]. According to a recent meta-analysis, significant seroprevalence were found in domestic animals including goats, sheep, cattle, dogs, pigs, chickens, mink, and geese and also in wild animals

including elk, deer, shrews. rodents, boars, hedgehogs, swan goose and doves[28]. SFTSV RNA was also detected, supporting the SFTSV animal transmission model in the wide spectrum of animal hosts[28]. However, vertical transmission between reservoir host animals and ticks has not clearly elucidated. Seroprevalence of SFTSV in human were also reported through a meta-analysis. The overall seroprevalence of anti-SFTSV antibodies among pooled 23,848 blood samples from healthy population in 7 provinces of China was 4.3%[29]. In South Korea, seroprevalence was 2.1%, but the correlation between SFTS case prevalence and seroprevalence remains to be clarified[30].

While SFTSV transmission in animals commonly occurs by tick bites, cases of human-to-human transmission through contact with blood or body fluid, including infections in healthcare workers from patients were reported and these facts posed a further threat to the public in East Asia[31,32].

1.3 Pathogenesis and clinical features of SFTS

1.3.1 Pathogenesis

Autopsy cases and histopathologic findings of SFTS patients showed that necrotizing lymphadenitis of systemic lymphoid tissues especially on the regional lymph nodes of tick bites[33–35]. Pancytopenia, especially thrombocytopenia is major feature of SFTS. In this regard, SFTSV-infected cells and macrophages are frequently seen in spleen and bone marrow with hemophagocytosis in bone marrow and ischemia of spleen, respectively. Also, extensive liver necrosis is commonly observed with aberrantly high serum levels of alanine aminotransferase (ALT), aspartate aminotransferase (AST), lactate dehydrogenase (LDH), and creatine phosphokinase (CPK) showing serious damage of liver in fatal SFTS cases[16,36].

Numerous features of pathologic findings in human cases were similarly recapitulated in murine mouse models. In SFTSV infected C57BL/6 mouse model, thrombocytopenia and leukopenia in accordance with histopathological changes in the spleen and bone marrow in the early phase of infection were demonstrated[37]. Lymphocyte depletions and colocalization of platelets in the cytoplasm of splenic macrophages in the

red pulp area in spleen revealed that phagocytosis of SFTSV-bound platelets by macrophages caused thrombocytopenia in SFTS. In consequence, to compensate for the platelet depletion, an increase in the number of megakaryocytes was observed in bone marrow and spleen[37]. In late phase of SFTSV infection in mouse model, pathological lesions were observed in the liver and kidney. In liver, scattered necrosis with degeneration of hepatocytes were shown. In parallel, impaired glomerulus, congestion in Bowman's space, and mesangial thickening were observed in kidney[37,38]. However, in immunocompetent murine models, lethal outcomes were not developed, and viral RNA was detected only in the spleen, liver, and kidney.

In contrast, in interferon alpha/beta receptor knock-out (IFNAR-/-) mouse models, mortality was observed in SFTSV inoculated mice[38,39]. SFTSV RNA was detected in various time points in multiple organs including blood, brain, heart, intestine, kidney, liver, lung, and spleen[38]. Also, histiocytic necrotizing lymphadenitis in lymph node and spleen along with loss of lymphoid follicles or white pulps were characterized[39,40]. Additionally, SFTSV infection of reticular cells in lymphoid nodules of intestine showed similar manifestations observed in SFTS patients with gastrointestinal symptoms[38].

1.3.2 Clinial features

The major clinical features of SFTS include high fever (body temperature ≥38° C), fatigue, malaise, anorexia, nausea, vomiting, diarrhea, thrombocytopenia, leukocytopenia, and abdominal pain[41,42]. The typical courses of SFTS include the incubation stage, fever stage, multi organ failure (MOF) stage, and convalescence stage. The incubation period is known as 5–14 days. Depending on the route of infection or viral dose, the period changes[16,41]. The fever stage lasts for 5 to 11 days and can overlap with the MOF stage which lasts 7 to 14 days. After onset of illness, major symptoms such as high fever, gastrointestinal symptoms, and lymphadenopathy develop in SFTS patients followed by thrombocytopenia and leukopenia[41,43]. Main laboratory parameters found elevated includes ALT, AST, LDH, CK, and creatine kinase myocardial b fraction (CK-MB) [16,44].

In severe cases, SFTS can include central nervous system manifestations, hemorrhagic signs, and multiple organ dysfunction, which can lead to death[16,17,45–47]. Risk factors including sustained thrombocytopenia, high blood viral RNA copies, elevated AST were listed as indicators of poor clinical outcome[17,41]. In addition, recent study with sample size of more than 2000 patients noticed that SFTS patients with older age, male,

diarrhea, dyspnea, and hemorrhagic signs or neurological symptoms had a higher risk of death[47]. Also, as strong prediction markers of death in early stage of infection, abnormal LDH, AST, blood urea nitrogen concentrations and neutrophil percentage were classified[47].

1.4 Diagnosis and treatment for SFTS

1.4.1 Diagnosis

Diagnosis of SFTS is done on the basis of epidemiological aspects and laboratory tests. Epidemic season, geographical location, occupation, or history of tick bites can be epidemiological features for SFTS diagnosis[11,41]. Clinical manifestations of probable SFTS cases include acute onset of fever, gastrointestinal symptoms, bleeding, and laboratory data consisting of thrombocytopenia and leukocytopenia. Because patient symptoms of SFTS are non-specific, laboratory confirmation is needed for disease confirmation.

Until now, the laboratory diagnostic criteria for confirmation of SFTS case has no big difference among China, South Korea, and Japan. Laboratory methods for SFTS diagnosis include (i) detection of SFTSV RNA by PCR using specimens, commonly from blood, (ii)

seroconversion, or detection of IgM, or a four-fold increase of SFTSV specific IgG titer in paired serum samples by ELISA or neutralization test, (iii) isolation of SFTSV from patient samples[9,11,32].

Since early viral RNA detection, using the highly conserved region of SFTSV genome as a target, is highly sensitive and specific and also rapid compared to several serological methods, reverse transcriptase PCR is commonly used for laboratory diagnosis of SFTSV infection[48]. The reverse transcription loop-mediated isothermal amplification method has also been developed for more rapid test[49].

Although serum neutralization test is regarded as the gold standard among serological methods for detecting virus specific antibodies, it is expensive, laborious, and requires manipulation of live virus in laboratories with high-level biosafety facility and specialized staffs. As for other serological diagnosis, double-antigen sandwich ELISA system using recombinant SFTSV N protein has been developed[50].

1.4.2 Treatment

Since SFTSV is a novel virus, which only has been less than ten years from the time of the first report, no specific treatment for SFTS exists.

Therefore, no more than supportive and symptomatic therapies are available for SFTS patients.

Although ribavirin has been used for several viral hemorrhagic fevers including Lassa fever[51], Crimean-Congo hemorrhagic fever[52] and hemorrhagic fever with renal syndrome caused by Hantavirus infection[53], ribavirin treatment had no significant benefit on platelet counts nor virus copy number[36]. Besides, adverse effects associated with SFTS patients including anemia were reported[54]. In contrast, increased survival benefit of SFTS patients with a viral load less than 10^6 copies per mL was shown in the recent study[47]. Still, the effect of ribavirin for SFTV infection remains controversial.

1.5 Drug development for SFTS

No vaccines or therapeutics specific for SFTS have been approved for human use. Recently, a Phase 3 clinical trial of favipiravir (Avigan), a drug approved for the treatment of influenza virus infection in Japan, was initiated to expand its indication to SFTS treatment[55]. Monoclonal antibodies or convalescent sera from SFTS patients were tested to identify potential therapeutic intervention targets, resulting in the identification of SFTSV glycoproteins as molecules required for host cell entry[56,57] and

also as critical targets for virus neutralization through the development of humoral immunity. Both the Gn and Gc envelope glycoproteins of SFTSV are type I transmembrane proteins, and Gc is proposed to be a membrane fusion protein critical for SFTSV infection[58]. This has also been shown in Rift Valley fever virus (RVFV)[59], which is a well-known phlebovirus, whereas the function of Gn remains largely elusive across all other species in the genus *Phlebovirus*. The structure of the Gn head domain, which is composed of three subdomains, was resolved in SFTSV and RVFV[60]. However, the homology and arrangement within subdomains differ considerably between the two viruses, and the structure of the Gn stem domain still remains unknown. Moreover, the generation of an antibody for these targets in infected humans is rare, due to the presence of immunodominant decoy epitopes in the nucleoprotein[61], which is a common phenomenon in a pathogenic virus-infected host[62]. In animal models, however, the protective effect of human convalescent sera was shown, suggesting that antibody therapy is possible[63]. Thus far, MAb4-5 is the only human neutralizing monoclonal antibody reported, and it was developed using a combinatorial human antibody library from five patients[64]. MAb4-5 binds to domain III of

SFTSV Gn glycoprotein[60]. The neutralizing effect of MAb4-5 has been shown only in in vitro, and its in vivo efficacy remains to be shown.

1.6 Antibody therapeutics for viral diseases

1.6.1 Antibody discovery technologies for viral infections

Virus neutralizing antibodies have been isolated by various strategies including methods utilizing combinatorial display libraries[65,66], methods using the hybridoma technique[67], and single B cell cloning methods that commonly sort out memory B cells or plasma B cells[68-71].

Phage displayed antibody libraries have been an efficient and conventional way to develop virus neutralizing antibodies from naturally infected human donors, or immunized animals. Transcripts encoding variable regions of antibody from B cells were cloned and displayed as single chain fragments on filamentous phage. Then, virus specific antibodies were isolated by panning procedures using recombinant viral proteins. Up to now, several monoclonal antibodies discovered by phage display method have been examined in clinical trials in several viral diseases including influenza virus infection (Diridavumab) and Rabies virus infection (Foravirumab) [72]. Despite the proved methods for

antibody generation, antibody display libraries have limitations that make difficulties in finding natural form of antibodies against viruses, such as random paring of light chain and heavy chain variable regions, loss of characteristics (e.g. expression, binding) in bacteria or yeast systems, and requirement for well-defined recombinant proteins of virus envelope[72,73].

Recently, to cope with the endemics occurred by newly emerging viral pathogens, single B cell-based techniques are frequently used for monoclonal antibody discovery[72,74-77]. A technique that enables functional screening and cloning of a large number of single B cells were used in isolation of human immunodeficiency virus (HIV) broadly neutralizing antibodies[78]. Though the use of predefined viral antigen is not applicable for isolation of antibodies against novel viruses, flow cytometry mediated antigen-specific B cell sorting approach has been exploited in various antibody developments for viral infections[79}72].

1.6.2 Virus targeting monoclonal antibodies

Historically, antibodies from patients who recovered from viral infection have been used to treat new patients[80], purified intravenous immune globulin (IVIg) has also been used for various infectious diseases[81,82] and

commercially available antiviral monoclonal antibodies have been developed. To date, two monoclonal antibodies were approved for prophylactic or therapeutic use against viral infections. Palivizumab was approved for the prophylaxis of respiratory syncytial virus (RSV) infection, and ibalizumab-uiyk was recently approved for the treatment of human immunodeficiency virus (HIV)-infected patients. Also, a number of antiviral monoclonal antibodies are in development at clinical trial stages.

For transplant recipients or HIV infected patients who have compromised immune systems, more than two cytomegalovirus (CMV) targeting therpaies are in clinical trials with combinations of two monoclonal antibodies[73,83,84]. CSJ148 is a combination of two human monoclonal antibodies which were isolated from Epstein-Barr Virus (EBV) immortalized B cells of human donors[84]. Two monoclonal antibodies bind to the viral gB protein and gH protein. Similarly, RG7667 is combination of two antibodies, one was isolated from spleen cells of CMV seropositive human, and the other was isolated from a mouse hybridoma[83].

For influenza infections, as a concept of passive immunization utilizing broadly neutralizing antibodies, numerous antibodies are in development.

For example, MHAA4549A is a human plasmablast cell derived influenza A stalk region binding antibody, which is known to neutralize all influenza A strains reported[85]. For other anti-influenza virus antibodies, antibodies including Lesofavumab (Genentech), CT-P27 (Celltrion), CR8020 (Crucell), MEDI8852 (MedImmune) are in clinical development for treatment of influenza A or B virus infection[72].

In addition, multiple clinical trials are ongoing for treatment of HIV infected patients. Especially, broadly neutralizing antibodies binding to CD4 binding site of HIV gp120 envelope, such as VRC01[79] and 3BNC117[86], are actively being tested in Phase II development.

Also, for RSV targeting antibodies, one of which is already an approved for prophylaxis in infants, are in developments for better outcomes. Affinity matured version of antibody based on Palivizumab, Motavizumab and its half-life extended derivative are in clinical trials[87,88]. Other novel antibodies targeting RSV are also in clinical development[73].

2 Materials and methods

2.1 Ethics statements: human subjects and animal models

The studies involving recovered patient's blood samples were reviewed and approved by the Institutional Ethics Review Board of Seoul National University Hospital (IRB approval number: 1405-031-576). All of the patients were adults and submitted written informed consent. All animal studies were conducted in an Animal Biosafety Level 3 (ABSL-3) facility at the Institut Pasteur Korea according to the principles established by the Animal Protection Act and the Laboratory Animal Act in Republic of Korea. Interferon α/β receptor knockout (IFNAR1$^{-/-}$, A129) mice (B&K Universal, Hull, UK) were bred, raised, and genotyped at the Institut Pasteur Korea. All experimental procedures were reviewed and approved by the Institutional Animal Care and Use Committee at the Institut Pasteur Korea (Animal protocol number: IPK-17003-1).

2.2 Production of recombinant SFTSV Gn/Gc glycoprotein fusion proteins

The SFTSV Gn glycoprotein amino acid sequences of various isolates used in this study were retrieved from the Virus Pathogen Database and Analysis Resource (ViPR). To obtain SFTSV Gn glycoprotein ectodomain coding DNA strands, human codon optimized DNA sequences corresponding to amino acid sequences from 20 to 452 of GenBank Accession No. ADZ04471 (Strain HB29), ADZ04477 (Strain SD4), ADZ04486 (Strain AH 15), BAN58185 (Strain YG1), AGT98506 (Strain Gangwon/Korea/2012) were synthesized (GenScript, Piscataway, NJ, USA and Integrated DNA Technologies, Coralville, IA, USA). Human codon optimized DNA sequence of SFTSV Gc ectodomain of strain Gangwon/Korea/2012, corresponding to the sequence from 563 to 1035 of AGT98506, was also synthesized. For the overexpression and purification of recombinant SFTSV Gn/Gc glycoprotein ecotodomain fused to the fragment crystallizable (Fc) region of human immunoglobulin heavy constant gamma1 (IGHG1), termed Gn-Fc/Gc-Fc, or fused to the human immunoglobulin kappa constant region (IGKC), termed Gn-Cκ/Gn-Cκ, SFTSV Gn/Gc glycoprotein ectodomain encoding genes were cloned into the modified pCEP4 vector

(V04450, Invitrogen, Carlsbad, CA, USA) with a leader sequence of the human immunoglobulin kappa chain, two *Sfi*I restriction enzyme sites, and the Fc region of human IGHG1 or human immunoglobulin kappa constant region, as previously described[89,90]. Subsequently, the vectors were used to transfect HEK 293F (R79007, Invitrogen) or Expi293F cells (A14527, Invitrogen) using polyethylenimine (23966-1; Polysciences, Warrington, PA, USA), then the transfected cells were cultured in FreeStyle 293 expression medium (12338026; Gibco, Thermo Fisher Scientific, Waltham, MA, USA). Overexpressed recombinant SFTSV Gn and Gc glycoprotein fusion proteins were purified by affinity chromatography using MabSelect or KappaSelect columns with the ÄKTA Pure chromatography system (11003495, 17545811, 29018225; GE Healthcare, Chicago, IL, USA), following the protocol provided by the manufacturer.

For alanine-scanning mutagenesis, SFTSV Gn glycoprotein with amino acid residues (315-389) substituted with alanine were produced by cloning synthesized DNA fragments (Integrated DNA Technologies) into a modified pCEP4 vector, as described above. Subsequently, influenza hemagglutinin (HA) tag sequence (YPYDVPDYA) was introduced to the C-terminus of the Fc region of human immunoglobulin heavy gamma1

and the whole protein, designated as Gn-Fc-HA, was produced as described above.

In order to produce histidine tagged SFTSV Gn glycoprotein, a ligand for surface plasmon resonance analysis, a Gn-Cκ with six carboxy-terminal poly-histidine residues was designed and produced as described above.

2.3 Human antibody library construction and antibody selection

Peripheral blood mononuclear cells of a patient who recovered from SFTS were collected using a Ficoll-Paque density gradient medium (17144002; GE Healthcare). Total RNA was isolated using TRIzol Reagent (15596018; Invitrogen), and cDNA was synthesized using a SuperScript III first-strand cDNA synthesis kit with oligo dT priming (18080051; Invitrogen). From this cDNA, a phage-display library of human single-chain variable fragments (scFv) was constructed, and four rounds of biopanning were performed to select scFv antibody clones from the library, as previously described[91,92]. For each round of biopanning, recombinant SFTSV Gn-Fc coated onto paramagnetic Dynabeads (14302D, Invitrogen) were used. To select SFTSV glycoprotein binding

clones, phage ELISA was performed as previously described, using Gn or Gc glycoprotein-coated microtiter plates, scFv displaying phages, and horseradish peroxidase (HRP) conjugated anti-M13 antibody (11973-MM05, Sino Biological, Beijing, China)[92]. The nucleotide sequences of positive scFv clones were determined by Sanger nucleotide sequencing (Cosmogenetech, Seoul, South Korea). Germline sequences of selected antibody variable regions were analyzed by the National Center for Biotechnology Information (NCBI) IgBLAST.

2.4 Production of single-chain variable fragment antibodies and IgG1 antibodies against SFTSV Gn glycoprotein

The genes encoding the variable heavy chain and variable light chain of Ab10 and MAb4-5[64] were synthesized (Integrated DNA Technologies, GenScript) and fused with the human heavy chain constant region gene (IgG_1) and human kappa light chain gene, and then cloned into an eukaryotic expression vector, as described previously[93,94]. The expression vectors were transfected into HEK 293F cells. The IgG_1 molecule was purified from the culture supernatant by affinity chromatography using MabSelect as described above. Genes encoding the scFv-Fc fusion

protein and the scFv-Cκ fusion protein were synthesized and cloned into a pCEP4 vector (Invitrogen). After transfection into HEK 293F cells, the recombinant proteins were overexpressed and purified as described above.

2.5 SFTSV preparation and immunofluorescent imaging-based neutralization test

The SFTSV strain of Gangwon/Korea/2012[12] was propagated in Vero cells (10081, Korean Cell Link Bank) with Roswell Park Memorial Institute (RPMI)-1640 medium (LM 011-01; Welgene, Daegu, South Korea) supplemented with 2% heat-inactivated fetal bovine serum (16000044; Gibco) and penicillin-streptomycin (10378016; Gibco). The fifty-percent tissue culture infective dose ($TCID_{50}$) values were titrated on Vero cells using the Reed-Muench method[67]. Ab10 or MAB4-5 scFv-Fc fusion protein was serially diluted in 10-fold increments from a 50 μg/mL concentration, then mixed with an equal volume of 100 $TCID_{50}$ SFTSV and incubated at 37 °C for 1 h. The virus-antibody mixture was transferred onto Vero cells in 8-well chamber slides (154534; Thermo Scientific, Waltham, MA, USA) and incubated at 37 °C for 1 h. For the no-infection-control group, no virus was added to the cells. In

contrast, for the infection-control group, no antibody was incubated with the virus. After removing the virus-antibody mixture, cells were cultured for 2 days. For the IFA, cultured cells were fixed with 4% paraformaldehyde in PBS for 1 h at room temperature. Slides were blocked and permeabilized with PBS containing 0.1% Triton X-100 and 1% bovine serum albumin, followed by incubation with 5 μg/mL of anti-SFTSV Gn glycoprotein antibody[35] at 4 °C overnight. After washing, cells were incubated for 1 h at room temperature with 1:100 diluted fluorescein isothiocyanate (FITC)-conjugated anti-rabbit IgG Fc antibody (111-095-046; Jackson ImmunoResearch, West Grove, PA, USA). To stain the nucleus, 4',6-diamidino-2-phenylindole dihydrochloride (DAPI) was used. Fluorescence image of cells was monitored under a confocal laser scanning microscope (TCS SP8; Leica, Wetzlar, Germany).

2.6 *In vivo* efficacy test

For animal experiments, the titer of SFTSV was measured by plaque forming assays[95]. Ten-fold serial dilutions of SFTSV were inoculated onto monolayers of Vero cells in 6-well tissue culture plates for 1 h at room temperature. After removal of the virus, cells were washed three

times with PBS and incubated with Dulbecco's Modified Eagle's Medium (12100-046; Gibco) based overlay medium containing 0.7% agar (214010; BD Biosciences, San Jose, CA, USA) for 7 days. For visualization of plaques, the overlay medium was removed, and the cells were fixed with 4% paraformaldehyde in PBS, followed by staining with 0.05% (w/v) crystal violet solution (C0775; Sigma-Aldrich, St. Louis, MO USA). Either 2 or 20 plaque forming units (PFU) of Gangwon/Korea/2012 strain SFTSV in 200 μL of PBS were inoculated in 8- to 10-week-old male or female A129 mice by a subcutaneous (s.c.) injection route. After 1 h of infection, mice were administered with Ab10 IgG_1 antibody or a PBS vehicle control through an intraperitoneal (i.p.) injection route, at 30 mg/kg of body weight for every 24 h for a consecutive 4 days. Palivizumab (MedImmune, Gaithersburg, MD, USA) or Mab4-5 IgG_1 was used as an isotype control or a positive control antibody, respectively. In the delayed treatment model, the infected mice were treated with antibodies at 1, 3, 4, or 5 days post-infection (d.p.i) for 4 days consecutively. Body weight and survival of mice were monitored until 10 days post-infection.

2.7 Enzyme-linked immunosorbent assays

In order to measure the binding activities of the Ab10 and MAb4-5 IgG_1 antibodies, 96-well half-area microplates (3690; Corning, Corning, NY, USA) were coated with Gn-Fc fusion protein and incubated at 4 °C overnight. Plates were blocked with 3% skim milk in PBS for 1 h at room temperature. The plates were then washed with PBS and received antibodies that were 10-fold serially diluted from 1 μM to 10 μM in blocking buffer. The plates were then incubated for 2 h at room temperature and washed three times with 0.05% Tween20 in PBS solution. Then, 50 μL of HRP-conjugated anti-human Ig kappa light chain antibody (AP502P; Chemicon, Temecula, CA, USA) diluted in blocking buffer (1:5000) was added into each well. Then, plates were incubated for 1 h at room temperature. After washing, each well received 50 μL of 3,3′,5,5′-tetramethylbenzidine (TMB) substrate solution (34028; Thermo Scientific). The color reaction was stopped by adding 50 μL of 2 M sulfuric acid. The absorbance of each well was measured at 450 nm using a microplate spectrophotometer (Multiskan GO; Thermo Scientific).

2.8 Surface plasmon resonance analysis of Ab10

The kinetics of Ab10 and Gn glycoprotein binding were measured by surface plasmon resonance analysis, using a Biacore T200 instrument with sensor chip CM5, amine coupling kit, and his capture kit (28975001, 29149603, BR100050, 28995056; GE Healthcare). We followed the recommended manufacturer's protocol for the procedures and conditions of reaction buffers, flow times, flow rates, and concentration of analytes. Briefly, anti-histidine antibody was immobilized on an activated CM5 chip, followed by a deactivation step. Then, histidine tagged Gn-Cκ was injected over the flow cells prior to antibody injection. For the association step, all of the Ab10 IgG_1 antibody in PBS at concentrations of two-fold increments ranging from 1.25 nM to 80 nM was injected for 3 min. For the dissociation step, PBS containing 0.005% of Tween20 was injected for 5 min. After each dissociation step, chip regeneration was performed.

2.9 Conformational epitope mapping by crosslinking coupled mass spectrometry

The epitope of Ab10 antibody was first determined by analyzing the complex of Ab10 antibody and SFTSV Gn-Cκ antigen linked with deuterated cross-linkers (CovalX, Zürich, Switzerland), as previously

described[96]. Briefly, antibody, antigen, and antibody/antigen complexes were characterized by high mass matrix-assisted laser desorption/ionization (MALDI) mass spectrometry using a MALDI TOF/TOF tandem mass spectrometer (Autoflex III; Bruker, Billerica, MA, USA) equipped with an interaction module (HM4; CovalX, Zürich, Switzerland). Afterwards, the antibody/antigen complex was crosslinked with DSS d0/d12 isotope-labeled homobifunctional N-hydroxysuccinimide esters, followed by reduction alkylation using dithiothreitol, iodoacetamide, and urea. To digest the reduced complex, a proteolytic buffer composed of trypsin, chymotrypsin, endoproteinase Asp-N, elastase, and thermolysin was used. The sample was then analyzed by nano-liquid chromatography (Ultimate 3000; Dionex, Sunnyvale, CA, USA) and Orbitrap mass spectrometry (Q Exactive Hybrid Quadrupole-Orbitrap; Thermo Scientific).

2.10 ELISA for epitope mapping

To measure the binding activities of Ab10 to mutated Gn, Ab10 scFv-Cκ antibody and an anti-influenza virus hemagglutinin antibody (clone 12CA5; Bio X Cell, Lebanon, NH, USA) were coated on a microplate, in parallel. Then, plates were blocked with 3% skim milk in PBS for 1 h

at room temperature. Transiently transfected cell supernatant containing recombinant Gn-Fc-HA proteins with alanine substitution was added to each well. After incubation for 2 h at room temperature, the microplate was washed three times with 0.05% Tween20 in PBS solution. Then, HRP-conjugated anti-human IgG Fc antibody (31423; Invitrogen) diluted in blocking buffer was added to each well. The plate was incubated for 1 h at room temperature. After washing, each well received 50 μL of 3,3′ ,5,5′ -tetramethylbenzidine (TMB) substrate solution (34028; Thermo Scientific). The color reaction was stopped by adding 50 μL of 2 M sulfuric acid. The absorbance of each well was measured at 450 nm using a microplate spectrophotometer (Multiskan GO; Thermo Scientific). Relative reactivity was calculated using absorbance values (Abs) as follows: % relative reactivity = [100 × {(Abs of mutant captured by Ab10) / (Abs of mutant captured by HA antibody)} / {(Abs of wildtype captured by Ab10) / (Abs of wildtype captured by HA antibody)}].

2.11 Data analysis

ELISA and IFA data including statistical comparisons were analyzed and graphed using GraphPad Prism software (San Diego, CA, USA).

Fluorescent signals measured by confocal microscopy were quantified using Leica Application Suite Advanced Fluorescence software. Mass spectrometry data were analyzed using XQuest and Stavrox software. Plasmon surface resonance data were analyzed using BIAevaluation software. Visualization, alignment, and phylogenic analyses of amino acid sequences were performed with Geneious software.

3 Results

3.1 Anti-Gn/Gc glycoprotein antibodies were selected from an antibody library generated from a convalescent SFTS patient.

In human embryonic kidney (HEK) 293F cells, we produced Gn and Gc glycoproteins fused with a crystallizable fragment of the human immunoglobulin (Ig) heavy chain constant region (Gn-Fc and Gc-Fc) or those fused with the human Ig kappa light chain constant region (Gn-Cκ and Gc-Cκ) and then purified the proteins by affinity chromatography. We constructed the phage-displayed single-chain variable fragment (scFv) antibody library with a complexity of 1.3×10^9 colony forming units using peripheral blood mononuclear cells isolated from a patient who had recovered from SFTS. The phage-display antibody library with a coverage level of 730× was subjected to four rounds of biopanning against either the recombinant Gn-Fc or the Gc-Fc fusion proteins conjugated to paramagnetic beads. We randomly selected phagemid clones from the output titer plate from the last round of biopanning and subjected these clones to phage enzyme-linked

immunosorbent assay (ELISA). To minimize the number of clones reactive to the Fc portion of fusion proteins, Gn-Cκ and Gc-Cκ were used as antigens. Positive clones were selected and subjected to Sanger sequencing to determine the scFv nucleotide sequence. We identified five clones reactive to Gn and five clones reactive to Gc. All of these scFv clones were expressed as a scFv antibody fused with Fc (scFv-Fc) in HEK293F cells and purified by affinity.

3.2 Ab10 mAb potently inhibited the amplification of SFTSV *in vitro*.

We tested 10 antibodies for their ability to reduce cytopathic effects (CPE) caused by SFTSV (Figure 1). One anti-Gn antibody, designated as Ab10, was extremely effective at neutralizing SFTSV, as shown by a reduction in the percentage of cells showing CPE from 90% to 10%. In the focus reduction neutralization test (FRNT), Ab10 also showed significantly higher potency compared to the other candidate antibodies (Figure 2). The V_H sequences of Ab10 had a 95.9% shared identity with the IGHV3-30*18 germline, excluding the heavy chain complementary determining region (HCDR) 3, whereas the V_κ sequence had 86.3% shared identity with the IGKV1-39*01 germline (Figure 3).

In an immunofluorescence assay (IFA) using Vero cells and an anti-Gn antibody, we determined the proportion of Gn glycoprotein producing cells, which were infected with SFTSV, to measure the neutralizing potency of Ab10. Only 5.6 ± 2.8% (mean ± s.d.) of Vero cells produced Gn glycoprotein when Ab10 was administered at a concentration of 50 μg/mL (956 nM) (Figure 4). When MAb4-5 antibody was applied at the same concentration, 77.8 ± 18.0% of the cells produced Gn glycoprotein. When cells were not protected by any antibody, all cells produced Gn glycoprotein and cells not incubated with SFTSV did not produce Gn glycoprotein.

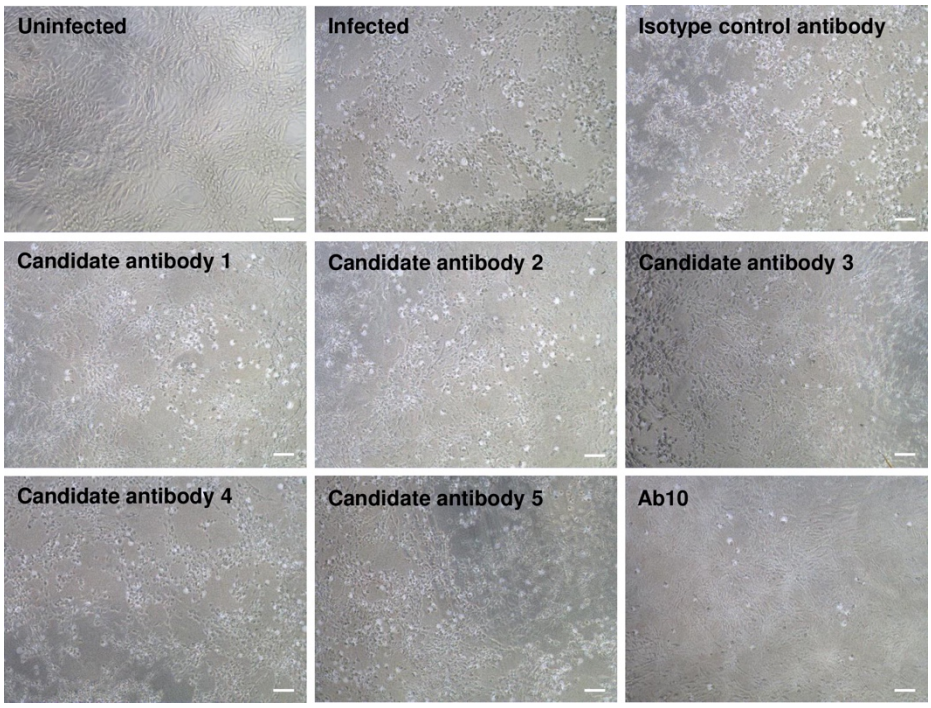

Figure 1. Inhibition of cytopathic effects of SFTSV

The cytopathic effects (CPE) of SFTSV on Vero cells were monitored to evaluate the protective effect of antibody clones. Candidate antibodies (scFv-Fc format) were mixed with 100 TCID50 of SFTSV (strain: Gangwon/Korea/2012) at a final concentration of 50 μg/mL and the mixtures were incubated for 1 h. SFTSV-antibody mixtures were then transferred to Vero cells at 80% confluency grown in 96-well tissue culture plates, and were incubated for 1 h. Then, cells were washed with PBS and incubated with fresh growth medium for 96 h. Cells were observed under a microscope to evaluate CPE and brightfield images are

shown (scale bar: 100 μm). In the control groups, cells not incubated with virus (Uninfected), cells infected without antibody treatment (Infected), cells incubated with virus, and the isotype control antibody (Isotype control antibody) were employed.

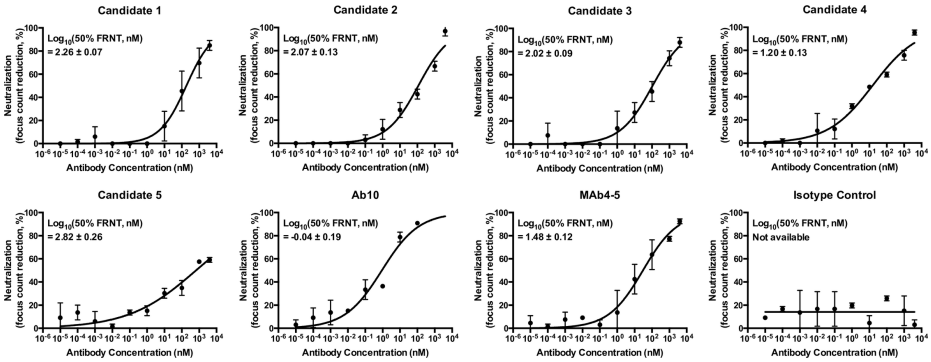

Figure 2. SFTSV focus reduction neutralization test of antibodies

Thirty to fifty focus forming units (FFU) of SFTSV were incubated with serially diluted scFv-Fc fusion proteins for 1 h at room temperature and transferred to Vero cells in a 24-well tissue culture plate. After incubation for 1 h at 37° C in a 5% CO2 incubator, the cells were overlaid with 0.5% methylcellulose in RPMI medium with 2% fetal bovine serum and cultured for 2 days. Cells were fixed with ice-cold methanol for 15 min and incubated with 1% bovine serum albumin in PBS for 1 h. Then, SFTSV localized clusters (foci) were visualized by incubating with 1 μg/mL of anti-SFTSV Gc glycoprotein antibody (Clone Ab3 from patent PCT/KR2017/003156) for 1 h, followed by incubation with 1:2,000 diluted goat anti-rabbit IgG Fc fragment specific antibody, conjugated with HRP (111-035-008; Jackson ImmunoResearch, West Grove, PA, USA) for 30 min and DAB substrate (K5007-BC; Dako). The percentage of neutralization was calculated for each diluted solution of

antibody as the percentage of decreased fraction in the number of foci compared to that of the virus without incubation of scFv-Fc fusion protein. An irrelevant scFv-Fc fusion protein was used as an isotype control. Dose-response curves were drawn by non-linear regression analyses (variable slope model) and 50% FRNT values were determined from graphs using GraphPad Prism6 software.

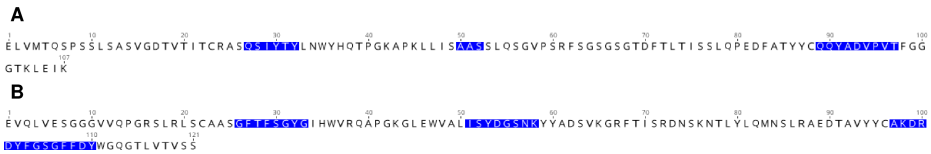

Figure 3. Amino acid sequences of Ab10 antibody variable region

The amino acid sequence of the light chain variable region (A) and heavy chain variable region (B) are shown. Blue letters indicate complementary determining regions (CDR) of each variable region defined by the International Immunogenetics Information System (IMGT).

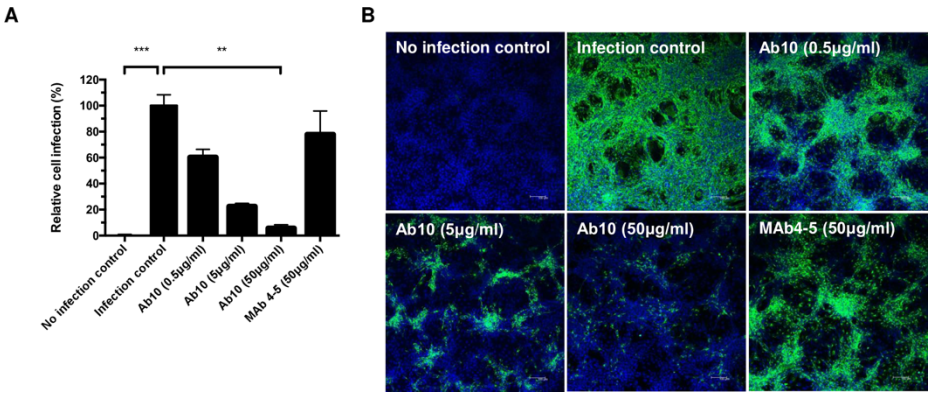

Figure 4. Ab10 has in vitro neutralizing activity against Severe Fever with Thrombocytopenia Syndrome virus (SFTSV)

To measure neutralizing efficacy, Ab10 scFv-Fc fusion protein was mixed with 100 TCID50 of SFTSV (strain: Gangwon/Korea/2012) and added to Vero cells. After incubation for 1 h, the cells were washed and cultured for 2 days. Then, the Gn glycoprotein produced in infected Vero cells was detected in an immunofluorescence assay using anti-SFTSV Gn glycoprotein antibody, which did not compete with Ab10 in its binding, with at least five technical replicates. The fluorescence signal intensity of stained SFTSV Gn glycoprotein was used as a quantitative indicator for viral infection. (A) The proportion of infected cells compared to non-treated cells was defined as relative cell infection (%) and was plotted. Mab4-5 scFv-Fc fusion protein was also treated in a parallel experiment. Error bars represent standard deviations (s.d), asterisks indicate a

statistically significant difference as determined by a nonparametric Friedman test with a post hoc Dunn's multiple comparison test (* $P \leq 0.05$, ** $P \leq 0.01$, *** $P \leq 0.001$, **** $P \leq 0.0001$). (B) Representative images of each treatment group are shown (scale bar, 100 μm). SFTSV Gn glycoprotein and nuclei were stained with FITC (green) and DAPI (blue), respectively.

3.3 Ab10 protected mice from SFTSV infection, even with treatment delayed up to 3 days.

For the animal study, the lethal dose of the Gangwon/Korea/2012 strain of SFTSV was determined in type I interferon (interferon α/β) receptor gene (IFNAR1)-deficient A129 mice (n = 4 per group). The mice were subcutaneously injected with a dose of either 20 or 2×10^5 plaque forming units (PFUs), and the mortality of mice was monitored (Figure 5). Because all mice died at 7 days post-infection (d.p.i.) even when injected with only 20 PFU, doses of 2 and 20 PFU were chosen for further studies.

Using the antibody protection model, A129 mice (n = 5 per group) were subcutaneously injected with the Gangwon/Korea/2012 strain of SFTSV at a dose of either 2 or 20 PFU. After 1 h, mice were intraperitoneally

administered with either phosphate-buffered saline (PBS), Ab10, MAb4-5, or a human IgG1 isotope control antibody at a dose of 600 μg (approximately corresponding to 30 mg/kg of body weight); for 4 days at 24 h intervals, the injection of the same amount of antibody was performed (Figure 6A).

In the groups treated with PBS or an isotype control antibody, all mice died within 7 days at both viral doses (Figure 6B and Figure 6C). At 4 d.p.i. with a dose of 2 PFU, approximately 10% of body weight was lost; at 3 d.p.i. with 20 PFU, 10-15% of body weight was lost. All mice treated with Ab10 survived both viral doses and did not have any weight loss. With MAb4-5 treatment, death occurred in all mice treated with a 2 PFU viral dose and in 80% of mice treated with a 20 PFU dose. Significant weight losses were also observed in all these mice.

In the delayed treatment model, the antibody treatment started from 1, 3, 4, or 5 d.p.i. and continued for 4 consecutive days (Figure 7A). At a 2 PFU viral dose, all mice survived when treatments with Ab10 were delayed until 3 d.p.i., and 80% survived when the treatments were delayed until 4 or 5 d.p.i. (Figure 7B and Figure 7C). Mice not treated until 4 d.p.i. had significant weight loss. At a 20 PFU viral dose, delaying Ab10 antibody treatment until 1 or 3 d.p.i. protected all or 80% of mice,

respectively. Mice with treatment delayed until 1 d.p.i. did not lose weight, whereas mice with treatment delayed until 3 d.p.i. lost 8% of their body weight. When treatment was delayed until 4 d.p.i. or later, all the mice died.

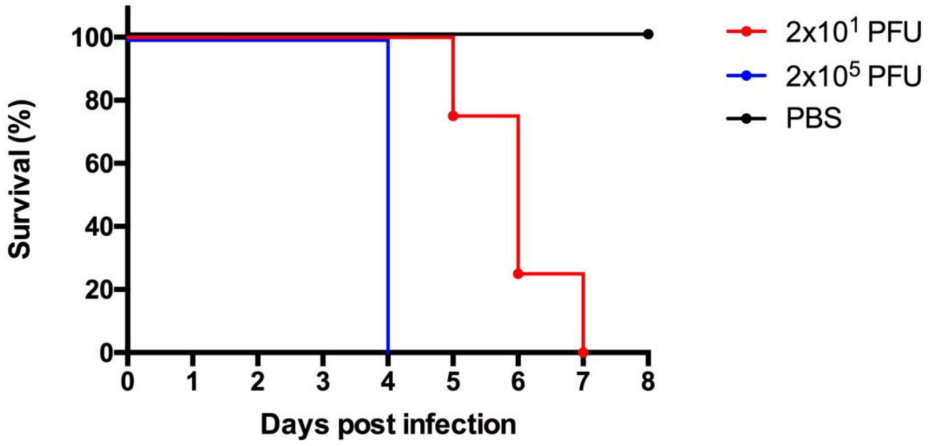

Figure 5. Survival of A129 mice infected with lethal doses of SFTSV

The 8-week-old A129 mice (n = 4 per group) were inoculated with 2×10^5 or 2×10^1 PFU of SFTSV (strain: Gangwon/Korea/2012) or PBS vehicle control using a subcutaneous route. The percentage survival was monitored daily until 8 days post-infection. Survival was determined by the Kaplan-Meier method.

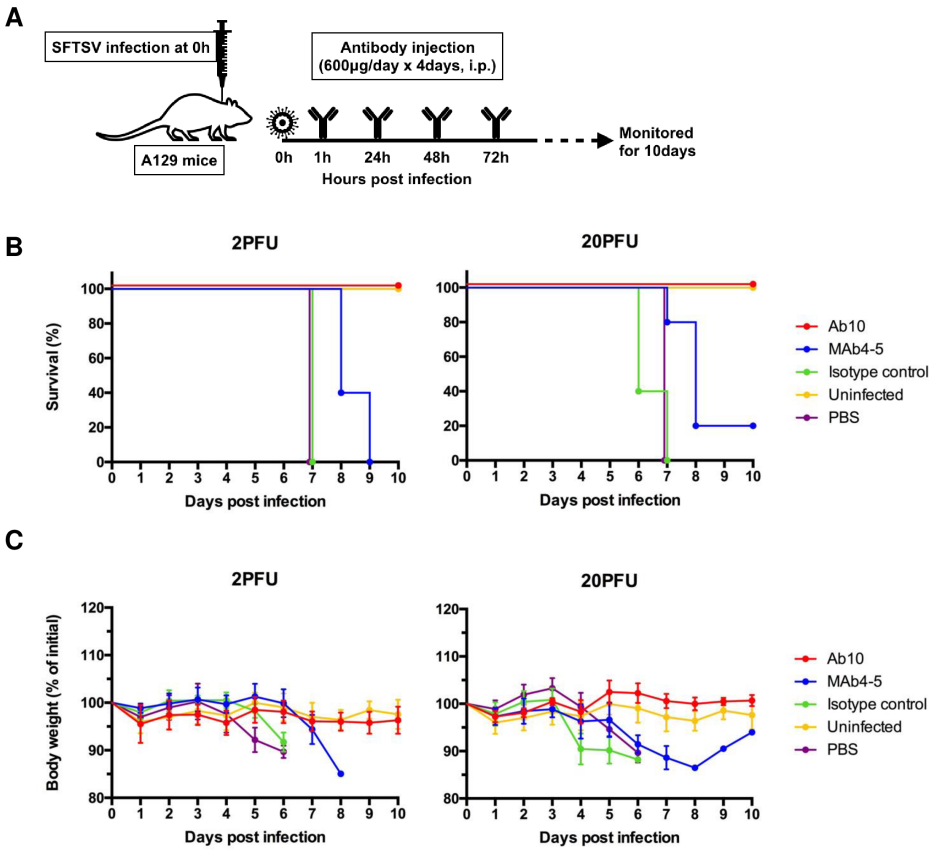

Figure 6. Ab10 protected mice from SFTSV infection

The overall scheme for the administration of virus and antibody is described in (A). Eight-week-old A129 mice (n = 5 per group) were inoculated with 2 or 20 PFU of SFTSV through a subcutaneous route. At 1, 24, 48, and 72 h post-infection, infected mice were intraperitoneally administered with 600 μg of Ab10, MAb4-5, IgG_1 isotype control antibody, or PBS vehicle control. Percentages of survival (B) and body weight relative to the day of virus inoculation (C) were monitored daily

until 10 days post-infection. Survival was determined by the Kaplan-Meier method. Relative body weight values in (C) are presented as the means with standard deviations of surviving mice in each group.

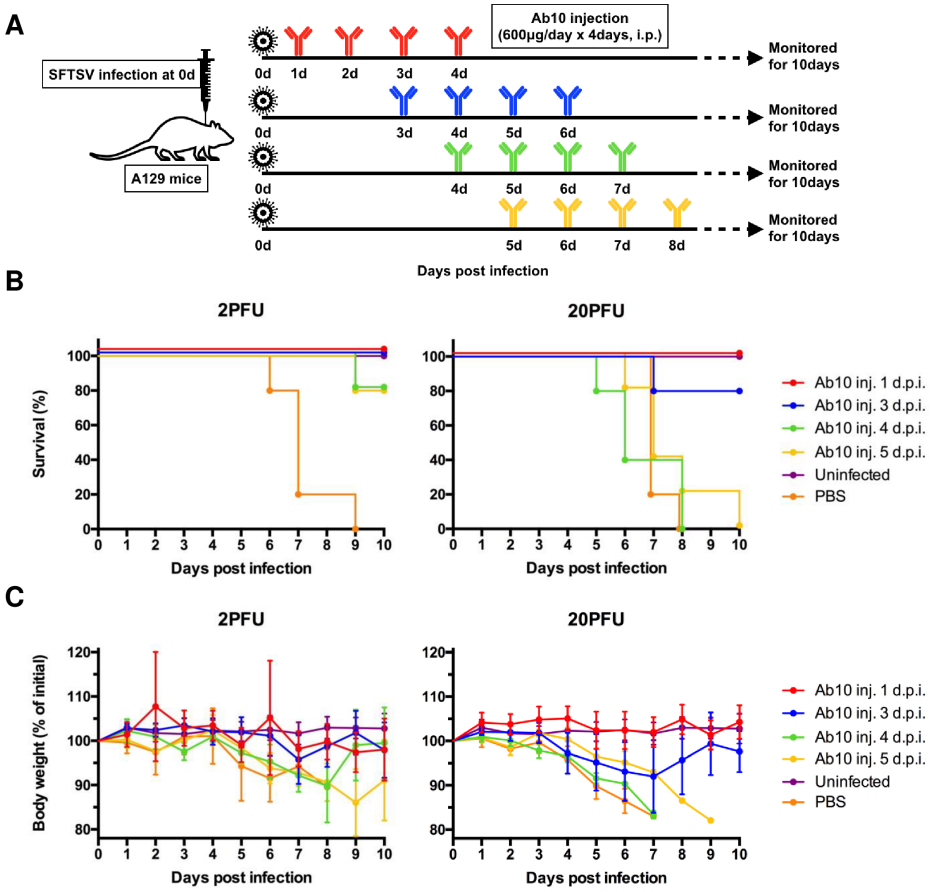

Figure 7. Delayed administration of Ab10 also protected mice from SFTSV infection up to 3 days after inoculation of the virus

The overall scheme for the virus challenge and delayed antibody administration is described in (A). Eight-week-old A129 mice (n = 5 per group) were inoculated with 2 or 20 PFU of SFTSV through a subcutaneous route. From 1, 3, 4, or 5 days post-infection, infected mice were intraperitoneally administered with 600 μg of Ab10 per day for 4 consecutive days. Percentages of survival (B) and weight relative to the

day of virus inoculation (C) were monitored daily until 10 days post-infection. Survival was determined by the Kaplan-Meier method. The values in (C) are presented as the means with standard deviations of surviving mice in each group.

3.4 Ab10 binds to recombinant Gn glycoprotein with high affinity in a broad variety of strains.

To check the reactivity of Ab10 to SFTSV strains other than Gangwon/Korea/2012, we overexpressed and purified recombinant Gn glycoproteins of other SFTSV strains. Binding of Ab10 to intact virus particles was also confirmed using an ELISA with a virus-coated microtiter plate (Figure 8). Among the 272 SFTSV strain sequences deposited in the Virus Pathogen Database and Analysis Resource (ViPR), we selected the strains HB29, AH15, SD4, and YG1, each belong to different clusters (Figure 9), to compare their reactivity with well-known virus isolates from China and Japan. We successfully overexpressed Gn glycoprotein from HB29 and SD4 as a Fc fusion protein and subjected these proteins to ELISAs. Ab10 IgG_1 successfully bound to Gn glycoproteins from the HB29 and SD4 strains in a dose-dependent manner at concentrations ranging from 10 pM to 1 nM (Figure 10A).

Additionally, the amount of antibody bound to the HB29 and SD4 Gn glycoproteins coated on the ELISA plate was higher than that of the Gangwon/Korea/2012 glycoproteins, at most of the tested concentrations. We also found that MAb4–5 was reactive to Gn glycoprotein from the HB29 and SD4 strains (Figure 10B).

We used surface plasmon resonance analyses to determine the kinetics of Ab10 binding to the Gn glycoprotein of Gangwon/Korea/2012. Ab10 bound to Gn glycoprotein with an equilibrium dissociation constant (K_D) of 104 pM and with an association rate (k_{on}) of $7.4 \times 10^5\ M^{-1}s^{-1}$ and a dissociation rate (k_{off}) of $7.7 \times 10^{-5}\ s^{-1}$ (Figure 10C).

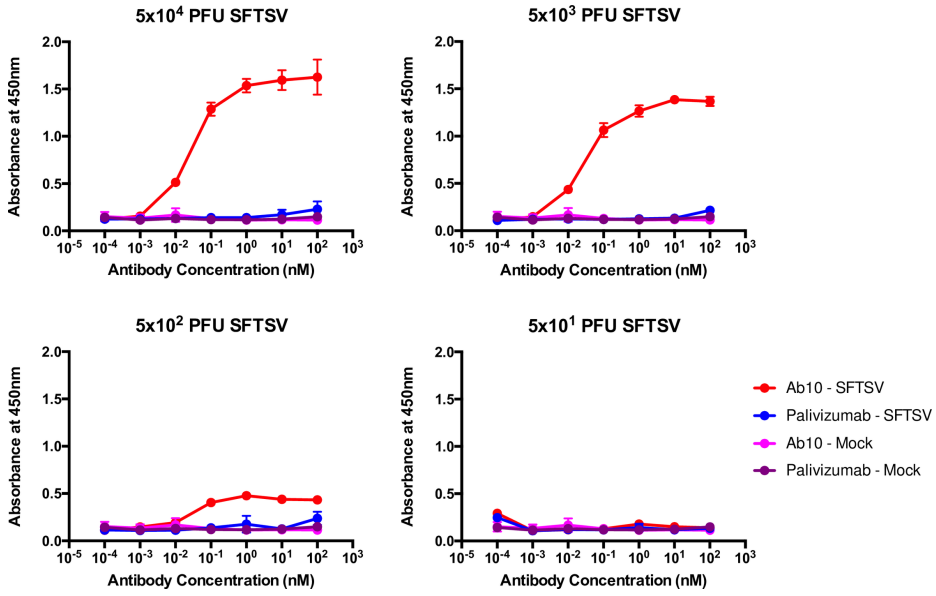

Figure 8. Dose-dependent binding of Ab10 to SFTSV

To examine binding activity of Ab10 antibody to SFTSV generated from Vero cells, serially diluted viral supernatants of SFTSV infected cells with a determined titer or the supernatant of mock-infected cells was coated onto microtiter plates (2692; Costar) at 4° C overnight. Fifty to five thousand PFU of SFTSV were used to coat each well. The plates were then incubated with serial dilutions of Ab10 antibody or Palivizumab as an isotype control, followed by HRP-conjugated anti-human IgG Fc antibody (31423; Invitrogen). Reactions were developed by adding TMB substrate (34028; Thermo Scientific) and were terminated by adding 2 M sulfuric acid. The absorbance was measured at 450 nm. The amount of virus coated on each microplate well is indicated on the top of each

graph, and the mean absorbance with standard deviation (s.d.) error bars is shown for each antibody concentration. Absorbance of Ab10 antibody bound to SFTSV-coated wells (red), Palivizumab bound to SFTSV-coated wells (blue), Ab10 antibody bound to mock-virus coated wells (magenta), and Palivizumab bound to mock-virus coated wells (purple) are shown in the graph.

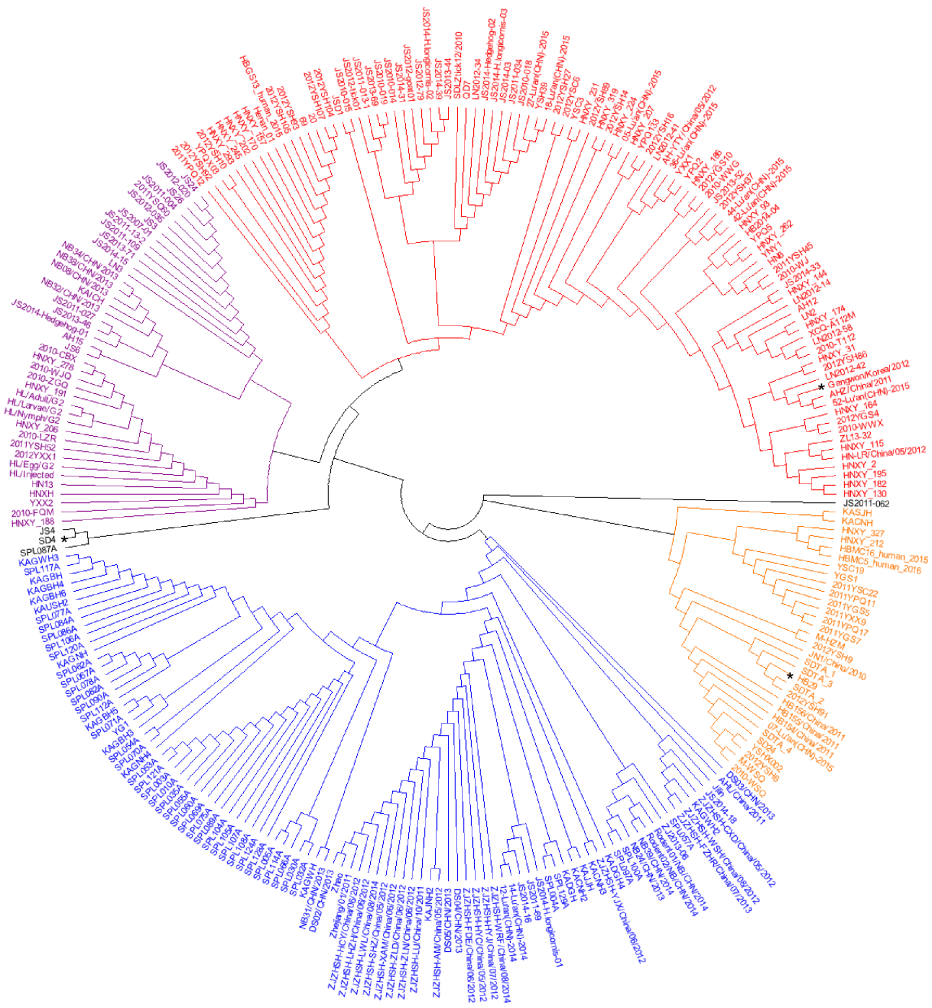

Figure 9. Phylogenetic analysis of SFTSV Gn glycoprotein ectodomain

The amino acid sequence of Gn glycoprotein from 272 SFTSV isolates deposited in ViPR were used for analysis. The sequences were trimmed to retain the amino acid residues from 20－452 that corresponded to the ectodomain. Trimmed sequences were analyzed, and a phylogenetic tree was built in a circular tree layout using the neighbor-joining method

with a Jukes–Cantor genetic distance model. The names of isolates are labeled beside the tip of each branch. Asterisks at the tip of branches indicate the isolates that were tested for binding activity of Ab10.

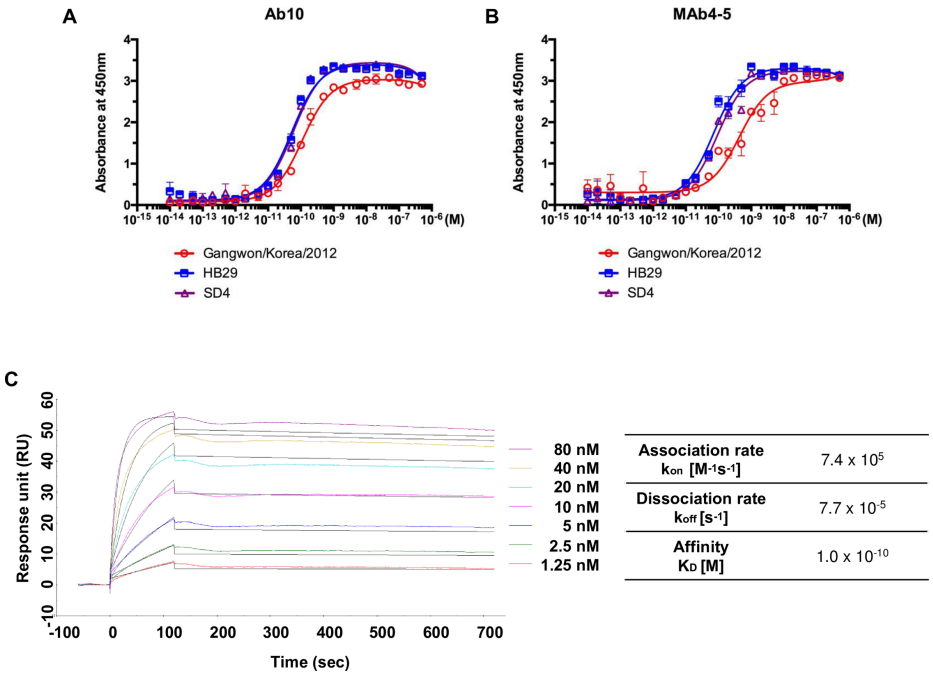

Figure 10. Ab10 also bound to Gn glycoprotein of HB29 and SD4 strains with comparable affinity to that of Gangwon/Korea 2012

Binding properties of human IgG1 monoclonal antibody Ab10 (A) and MAb4-5 (B) to the recombinant Gn glycoprotein ectodomain of Gangwon/Korea 2012, HB29, and SD4 strains were measured by enzyme-linked immunosorbent assay (ELISA). Non-linear regression curves were fitted to a one site specific saturation binding model and the mean absorbance at 450 nm with standard deviation (s.d.) error bars are shown at each antibody concentration. (C) Surface plasmon analysis of Ab10 antibody was performed on the CM5 chip with an immobilized

anti-histidine antibody binding to a poly-histidine tagged SFTSV Gn ectodomain. The experimental data at concentrations of 80, 40, 20, 10, 5, 2.5, and 1.25 nM Ab10 antibody are shown in color, and the fitted curves are shown in black. Calculated rate constants are shown in the table.

3.5 Ab10 binds to a non-linear epitope on domain II and the stem region of the Gn glycoprotein.

In an immunoblot analysis using recombinant Gn glycoprotein from the Gangwon/Korea/2012 strain, Ab10 did not react to Gn glycoprotein, whereas some other anti-Gn antibodies were reactive (Figure 11). Based on this observation, we assumed that the antibody reacted to a non-linear epitope.

To discover the site where Ab10 binds, we performed crosslinking coupled mass spectrometry using a deuterium isotope-labeled homo-bifunctional linker, which forms covalent bonds between amino acid residues within the interface of the antibody-antigen complex as described previously[96]. We found that cross-linkers bound to five amino acid residues (318Y, 324R, 326K, 328Y, and 331S) within domain II of

the SFTSV Gn glycoprotein and also to four amino acid residues (371K, 372S, 379H, and 383S) within the stem region (Figure 12A).

Based on this observation, we prepared several alanine-replacement mutants that spanned from 315V to 389K, and tested their reactivity to Ab10 using ELISAs. All the mutants were expressed with an HA peptide at the carboxy terminus and the tags were used to measure the relative amount of each mutant. Alanine mutant proteins were captured by the Ab10 antibody, which was coated on the ELISA plate. Then, we measured the amount of captured mutant proteins by detecting the Fc portion of protein. The signals detected by capturing the HA peptide were used to normalize expression of mutant proteins. We measured the reactivity of Ab10 to alanine mutant Gn proteins, relative to wild type Gn glycoprotein, and found that alanine replacement of the amino acid residues in domain II from V315 to M334 resulted in reduced relative reactivity of Ab10 by more than 60%, except for S317, G319, and M321. This finding was consistent with our results deduced from the crosslinking coupled mass spectrometry (Figure 12A and Figure 12B).

In the stem region, replacing the cystine residues (C349, C356, C376, and C381) reduced the relative reactivity by more than 80%. This observation was consistent with a previous report that the structural stability of Gn

was disrupted by a C356A mutation[60]. Also, mutation of the flanking residues of cystine, corresponding to G351, L354, E355, I357, T374, and V375 also reduced the reactivity by over 60%. Of the mutated residues that were distant from cysteine residues, mutation of G360, V361, R362, L363, T365, L370, G387, and K389 residues reduced the relative reactivity by more than 80%. The other mutations had minor effects on reactivity. Overall, Ab10 binding to Gn was predicted to be affected by 25 amino acid residues within domain II and the stem region of SFTSV Gn glycoprotein. Given that Gn glycoproteins from 247 isolates have conserved sequences for these 25 amino acid residues, we expect that Ab10 can react with 90.8% (247 out of 272) of SFTSV isolates currently reported (S8 Fig).

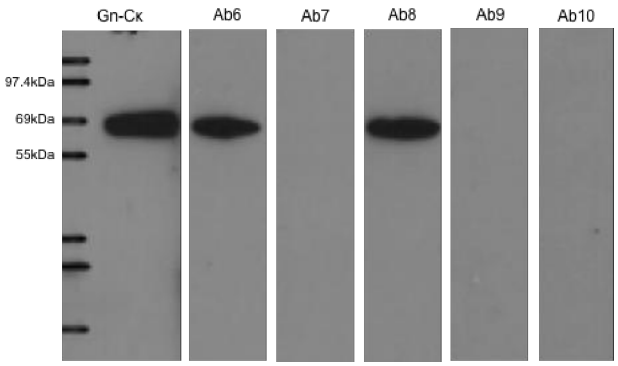

Figure 11. Immunoblot of recombinant Gn-Cκ fusion protein using anti-Gn antibodies

Recombinant SFTSV Gn-Cκ was prepared with sample buffer and reducing agent (NP0008 and NP0004; Invitrogen). The samples were then separated on a polyacrylamide gel (NP0321BOX; Invitrogen) by electrophoresis and transferred to a nitrocellulose membrane. After blocking with 5% (w/v) skim milk in Tris-buffered saline (pH 7.4) the membrane was incubated with 100 ng/mL of five (Ab6 to Ab10) SFTSV Gn specific antibodies in a scFv-Fc format. Gn bound antibodies were probed with HRP-conjugated anti-human IgG Fc antibody (31423; Invitrogen). To confirm the presence of Gn-Cκ protein, HRP-conjugated anti-human Ig kappa light chain antibody (AP502P, Chemicon, Temecula, CA, USA) was used to directly detect Gn-Cκ. The blots were visualized using a chemiluminescent substrate (34578; Thermo Scientific).

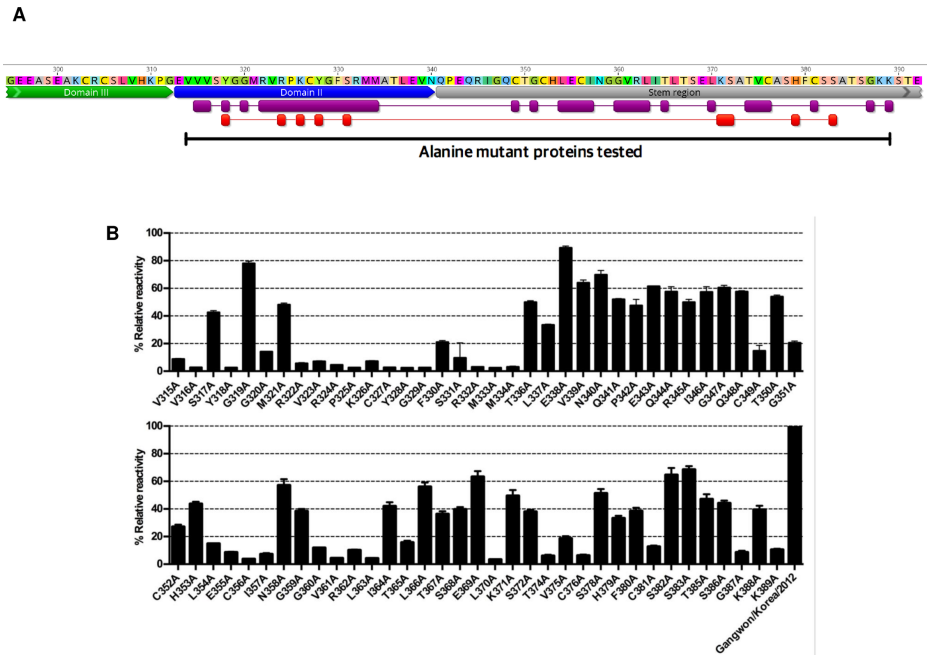

Figure 12. The epitope of Ab10 was determined by alanine mutant analysis

The conformational epitope of Ab10 antibody on the Gn glycoprotein ectodomain was determined by measuring antibody binding activity to recombinant mutant proteins with amino acid residues that were substituted with alanine at residues corresponding to 315–389. (A) Epitopes predicted by cross-linker assisted mass spectrometry are shown in red, and alanine substituted residues that affected Ab10 antibody binding are shown in purple. The overlapping domain II (blue annotation) and region upstream of the stem region (gray annotation) are also indicated. (B) The reactivity of Ab10 to each alanine mutant is

represented as relative reactivity, which was calculated using absorbance values (Abs) as follows: % Relative reactivity = [100 × {(Abs of mutant captured by Ab10) / (Abs of mutant captured by HA antibody)} / {(Abs of wildtype captured by Ab10) / (Abs of wildtype captured by HA antibody)}]. Bars indicate the mean and standard deviation (s.d.).

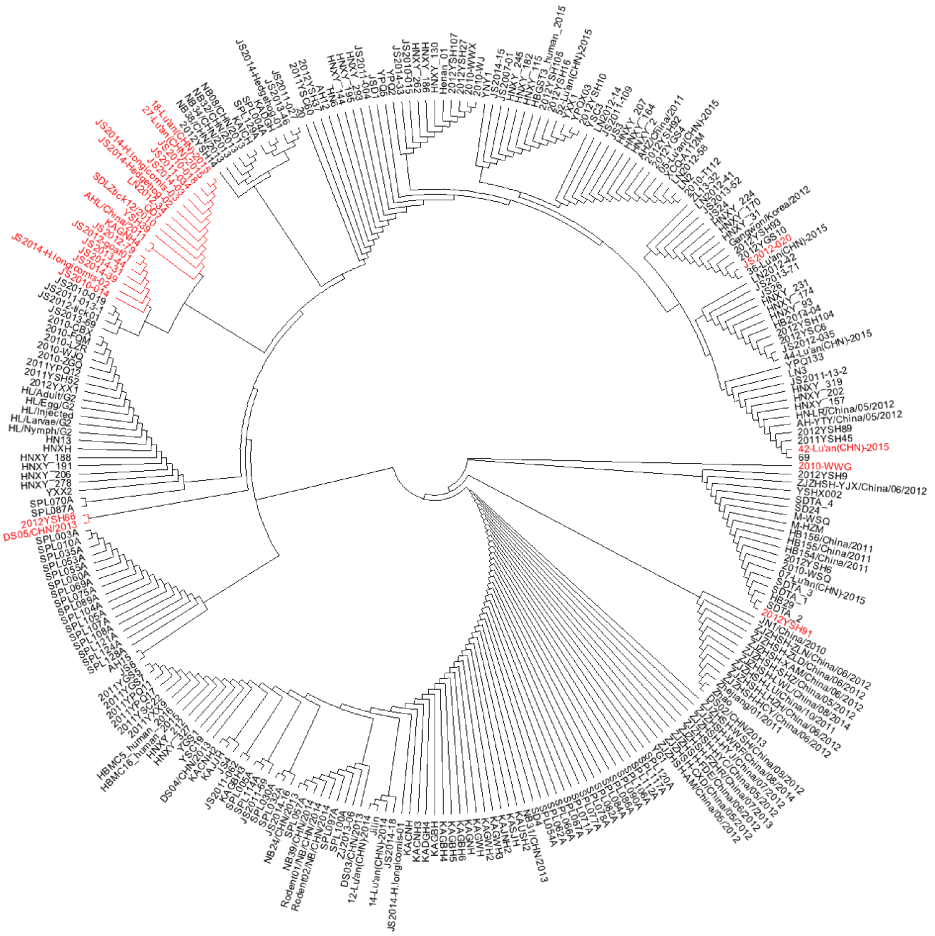

Figure 13. Phylogenetic analysis of sequences covering the Ab10 epitope

The amino acid sequence of Gn glycoprotein from the 272 SFTSV isolates deposited in ViPR were analyzed. The sequences were trimmed to retain the amino acids from 313–389 that correspond to the residues recognized by Ab10. Trimmed sequences were analyzed, and a phylogenetic tree was built in a circular tree layout using the neighbor-joining method with a Jukes-Cantor genetic distance model. The names of isolates are written

beside the tip of each branch. Strain names labeled in red indicate that the Gn glycoprotein of the indicated strain is predicted to not interact with Ab10.

4 Discussion

Antibodies play a pivotal role in preventing viral entry into cells and can induce lysis of infected cells through antibody-dependent cellular cytotoxicity or complement-dependent cytotoxicity[97-101]. Polysera from recovered patients or from vaccinated donors have been used as prophylactic agents for various viral diseases, including hepatitis B and rabies[72]. As an alternative approach, virus-directed monoclonal antibodies have also been developed and tested as therapies or as prophylaxis for viral diseases. Palivizumab (Synagis) was market-approved for the prophylaxis of RSV in 1998. In addition, antibodies against HIV[102-104], RSV[105], Ebola virus[106] and influenza virus[107,108] demonstrated potent efficacy in animal models. Antibodies targeting emerging or re-emerging viruses including MERS-CoV[74,109,110] and Zika virus[77,111,112] were also developed and are being tested in clinical trials. In the past several decades, antibodies have become one of the major therapeutic agents for cancer and autoimmune disease with indications that have rapidly broadened in recent years. Recent technical improvements in the discovery and manufacturing steps of therapeutic antibody production have also allowed rapid and successful antibody development to combat emerging infectious diseases[113].

Until now, SFTS patients have been reported from China, South Korea, and Japan, and the number of patients has increased each year[11,14,15]. However, SFTS fatality varies among the three countries[47]. The average case fatality rate in China from 2011 to 2016 was 6.40%[11]. Those in South Korea and Japan after 2013 were much higher; 20.9%[14] and 19.4%[15], respectively. In the Virus Pathogen Database and Analysis Resource (ViPR), 272 sequences of SFTSV isolates are currently deposited. However, it is unknown if there is any significant variability in the virulence of these isolates. Previous reports showed that mice died 5 to 7 days after infection with 10^6 focus forming units (FFU) of the YG1 strain[63] or 10^6 $TCID_{50}$ of the SPL010 strain[40]. Based on these observations, we first inoculated A129 mice with 2×10^5 PFU of the Gangwon/Korea/2012 strain and observed that all mice died 4 days after infection. With a 20 PFU dose of the Gangwon/Korea/2012 strain, mice died 5 to 7 days after infection. This increased virulence was also reported by a study that showed a similar fatality rate in STAT2 knockout Syrian hamsters challenged with 10 PFU of the HB29 strain[114].

We have also observed a discrepancy in the body weights at death between our study and that of another group. In our data, A129 mice died after losing 15% of their body weight. But in a study using the

SPL010 strain, mice died after losing 30% of their body weight[40]. Although only a few studies reported the mortality of mice exposed to SFTSV and the possibilities that differences in virus titer measurement methods obscure the comparison of outcomes could not be entirely excluded, these conflicting results might be due to a difference in virulence between the strains. Such differences in virulence between strains of the RVFV, a phlebovirus similar to SFTSV, have been reported[115]. Nevertheless, whether specific genetic lineages of SFTSV elicit the high lethality of mice has not proven, the high fatality rate in human cases calls for further studies concerning lineage-specific differences in virulence to forecast the severity of SFTSV infection in possible future outbreaks.

The mechanisms of antibody inhibition of viral replication inside host cells have been studied extensively, especially in the case of influenza virus. The most-widely known mechanism is binding of an antibody to the portion of the virus that interacts with the host cell receptor, thereby blocking the interaction between the virus and the host cell[116]. Another group of antibodies was reported to bind the stem region of influenza hemagglutinin that is critical for conformational rearrangements that occur during membrane fusion[117-119]. This mechanism has more potential

to be utilized for clinical development, because the stem region has fewer mutations than the receptor binding site. Additionally, several groups, including ours, have elucidated unconventional virus neutralizing mechanisms that affect the infection steps that occur after membrane fusion[120,121].

In our crosslinking coupled mass spectrometry and alanine mutant studies, the Ab10 epitope was confined to domain II and the stem region of the Gn glycoprotein. Although the crystal structure of the phlebovirus Gn glycoprotein stem region has not yet been solved, a recent report showed a cryo-electron microscopy map of RVFV, and depicted the crystal structure of the RVFV Gn glycoprotein head region without a stem region[122]. The report also describes the membrane fusion mechanism of RVFV that is mediated by a low pH-induced exposure of the hydrophobic Gc fusion loop. At a neutral pH, the Gn domain II (β-ribbon domain) shields the Gc fusion loop in the pre-fusion state and prevents premature fusion. Based on this report, we hypothesize that Ab10 simultaneously binds to domain II and the stem region of the Gn glycoprotein and prevents un-shielding of the Gc fusion loop.

In conclusion, Ab10 is a monoclonal antibody that has shown therapeutic efficacy in a mouse SFTSV infection model. Although the

neutralization efficacy of Ab10 was only tested in the Gangwon/Korea/2012 strain that was cultured in Vero cells, we confirmed its binding capability to recombinant SFTSV Gn in the HB29 and SD4 strains, which are both from China. According to the epitope revealed in this study, Ab10 is estimated to interact with the majority of SFTSV isolates currently reported. Based on these results, we believe that Ab10 has sufficient potential to be developed as a prophylactic and therapeutic agent for a broad variety of SFTS isolates.

Further development of this monoclonal antibody beyond the proof of concept would begin with physicochemical evaluations required for the decision making on whether the antibody is feasible enough for the high-cost large scale manufacturing. Multiple requirements for the clinical development of a monoclonal antibody include high expression yield, high solubility, low heterogeneity, high conformational stability, low immunogenicity, high specificity, et cetera. Other than sufficing properties related to chemical characteristics and manufacturing, preclinical pharmacology and toxicology studies are mandatory for the first-in-human trial. Notably, the study of pharmacokinetics and pharmacodynamics of the antibody in appropriate animal models generally precedes for the selection of effective and safe dose in humans.

Dose solution analysis, ELISA based immunogenicity assays, and pharmacodynamics assays are required in common.

5 References

1. Adams, M. J. *et al.* Changes to taxonomy and the International Code of Virus Classification and Nomenclature ratified by the International Committee on Taxonomy of Viruses (2017). *Arch Virol* **162**, 2505 – 2538 (2017).

2. King, A. M. Q. *et al.* Changes to taxonomy and the International Code of Virus Classification and Nomenclature ratified by the International Committee on Taxonomy of Viruses (2018). *Arch Virol* **163**, 2601 – 2631 (2018).

3. Liu, S. *et al.* Systematic review of severe fever with thrombocytopenia syndrome: virology, epidemiology, and clinical characteristics. *Rev. Med. Virol.* **24**, 90 – 102 (2014).

4. Liu, L., Chen, W., Yang, Y. & Jiang, Y. Molecular evolution of fever, thrombocytopenia and leukocytopenia virus (FTLSV) based on whole-genome sequences. *Infection, Genetics and Evolution* **39**, 55 – 63 (2016).

5. Zhan, J. *et al.* Current status of severe fever with thrombocytopenia syndrome in China. *Virologica Sinica* **32**, 51 – 62 (2017).

6. Fu, Y. *et al.* Phylogeographic analysis of severe fever with thrombocytopenia syndrome virus from Zhoushan Islands, China: implication for transmission across the ocean. *Sci Rep* **6**, 19563 (2016).

7. He, C.-Q. & Ding, N.-Z. Discovery of severe fever with thrombocytopenia syndrome bunyavirus strains originating from intragenic recombination. *Journal of Virology* **86**, 12426 – 12430 (2012).

8. Robles, N. J. C., Han, H. J., Park, S.-J. & Choi, Y. K. Epidemiology of severe fever and thrombocytopenia syndrome

virus infection and the need for therapeutics for the prevention. *Clinical and Experimental Vaccine Research* **7**, 43–50 (2018).

9. Yu, X.-J. *et al.* Fever with Thrombocytopenia Associated with a Novel Bunyavirus in China. *N Engl J Med* **364**, 1523–1532 (2011).

10. Xu, B. *et al.* Metagenomic analysis of fever, thrombocytopenia and leukopenia syndrome (FTLS) in Henan Province, China: discovery of a new bunyavirus. *PLoS Pathog.* **7**, e1002369 (2011).

11. Sun, J. *et al.* The changing epidemiological characteristics of severe fever with thrombocytopenia syndrome in China, 2011–2016. *Sci Rep* **7**, 9236 (2017).

12. Kim, K.-H. *et al.* Severe fever with thrombocytopenia syndrome, South Korea, 2012. *Emerging Infect. Dis.* **19**, 1892–1894 (2013).

13. Takahashi, T. *et al.* The first identification and retrospective study of Severe Fever with Thrombocytopenia Syndrome in Japan. *J. Infect. Dis.* **209**, 816–827 (2014).

14. Korea Centers for Disease Control and Prevention. Disease information (Severe Fever with Thrombocytopenia Syndrome, SFTS). *cdc.go.kr* (2018). Available at: http://www.cdc.go.kr/CDC/health/CdcKrHealth0101.jsp?menuIds=HOME001-MNU1132-MNU1147-MNU0746-MNU2423&fid=7956&cid=70361. (Accessed: 12 April 2019)

15. National Institute of Infectious Diseases, Japan. Severe Fever with Thrombocytopenia Syndrome (SFTS). *niid.go.jp* (2018). Available at: https://www.niid.go.jp/niid/ja/diseases/sa/sfts.html. (Accessed: 15 August 2018)

16. Gai, Z.-T. *et al.* Clinical Progress and Risk Factors for Death in Severe Fever with Thrombocytopenia Syndrome Patients. *J. Infect. Dis.* **206**, 1095–1102 (2012).

17. Zhang, Y.-Z. *et al.* Hemorrhagic fever caused by a novel Bunyavirus in China: pathogenesis and correlates of fatal outcome. *Clin. Infect. Dis.* **54**, 527–533 (2012).

18. Liu, K. *et al.* A National Assessment of the Epidemiology of Severe Fever with Thrombocytopenia Syndrome, China. *Sci Rep* **5**, 9679 (2015).

19. Ding, F. *et al.* Epidemiologic Features of Severe Fever With Thrombocytopenia Syndrome in China, 2011–2012. *Clin. Infect. Dis.* **56**, 1682–1683 (2013).

20. Yu, X.-J. Risk factors for death in severe fever with thrombocytopenia syndrome. *Lancet Infect Dis* **18**, 1056–1057 (2018).

21. Zhang, Y.-Z. *et al.* The ecology, genetic diversity, and phylogeny of Huaiyangshan virus in China. *Journal of Virology* **86**, 2864–2868 (2012).

22. Yun, S.-M. *et al.* Severe Fever with Thrombocytopenia Syndrome Virus in Ticks Collected from Humans, South Korea, 2013. *Emerging Infect. Dis.* **20**, 1358–1361 (2014).

23. Rainey, T., Occi, J. L., Robbins, R. G. & Egizi, A. Discovery of Haemaphysalis longicornis (Ixodida: Ixodidae) Parasitizing a Sheep in New Jersey, United States. *J Med Entomol* **55**, 757–759 (2018).

24. Li, D. A highly pathogenic new bunyavirus emerged in China. *Emerging Microbes & Infections* **2**, e1 (2013).

25. Zhang, Y.-Z. & Xu, J. The emergence and cross species transmission of newly discovered tick-borne Bunyavirus in China. *Current Opinion in Virology* **16**, 126–131 (2016).

26. Zhao, L. *et al.* Severe fever with thrombocytopenia syndrome virus, Shandong Province, China. *Emerging Infect. Dis.* **18**, 963–965 (2012).

27. Niu, G. *et al.* Severe fever with thrombocytopenia syndrome virus among domesticated animals, China. *Emerging Infect. Dis.* **19**, 756–763 (2013).

28. Chen, C. *et al.* Animals as amplify hosts in the spread of severe fever with thrombocytopenia syndrome virus A systematic review and meta-analysis. *International Journal of Infectious Diseases* **79**, 77–84 (2019).

29. Li, P. *et al.* Seroprevalence of severe fever with thrombocytopenia syndrome virus in China: A systematic review and meta-analysis. *PLoS ONE* **12**, e0175592 (2017).

30. Kim, K.-H., Ko, M. K., Kim, N., Kim, H. H. & Yi, J. Seroprevalence of Severe Fever with Thrombocytopenia Syndrome in Southeastern Korea, 2015. *J. Korean Med. Sci.* **32**, 29–32 (2017).

31. Liu, Y. *et al.* Person-to-person transmission of severe fever with thrombocytopenia syndrome virus. *Vector Borne Zoonotic Dis.* **12**, 156–160 (2012).

32. Gai, Z. *et al.* Person-to-Person Transmission of Severe Fever With Thrombocytopenia Syndrome Bunyavirus Through Blood Contact. *Clin. Infect. Dis.* **54**, 249–252 (2012).

33. Hiraki, T. *et al.* Two autopsy cases of severe fever with thrombocytopenia syndrome (SFTS) in Japan: a pathognomonic histological feature and unique complication of SFTS. *Pathol. Int.* **64**, 569–575 (2014).

34. Uehara, N., Yano, T., Ishihara, A., Saijou, M. & Suzuki, T. Fatal Severe Fever with Thrombocytopenia Syndrome: An Autopsy Case Report. *Intern. Med.* **55**, 831–838 (2016).

35. Kang, C. K. *et al.* 18F-FDG PET and histopathologic findings in a patient with severe fever with thrombocytopenia syndrome. *Ticks and Tick-borne Diseases* **9**, 972 – 975 (2018).

36. Liu, W. *et al.* Case-fatality ratio and effectiveness of ribavirin therapy among hospitalized patients in china who had severe fever with thrombocytopenia syndrome. *Clin. Infect. Dis.* **57**, 1292 – 1299 (2013).

37. Jin, C. *et al.* Pathogenesis of emerging severe fever with thrombocytopenia syndrome virus in C57/BL6 mouse model. *Proc. Natl. Acad. Sci. U.S.A.* **109**, 10053 – 10058 (2012).

38. Liu, Y. *et al.* The pathogenesis of severe fever with thrombocytopenia syndrome virus infection in alpha/beta interferon knockout mice: insights into the pathologic mechanisms of a new viral hemorrhagic fever. *Journal of Virology* **88**, 1781 – 1786 (2014).

39. Matsuno, K. *et al.* Animal Models of Emerging Tick-Borne Phleboviruses: Determining Target Cells in a Lethal Model of SFTSV Infection. *Front. Microbiol.* **8**, 8172 (2017).

40. Tani, H. *et al.* Efficacy of T-705 (Favipiravir) in the Treatment of Infections with Lethal Severe Fever with Thrombocytopenia Syndrome Virus. *mSphere* **1**, e00061 – 15 (2016).

41. Liu, Q., He, B., Huang, S.-Y., Wei, F. & Zhu, X.-Q. Severe fever with thrombocytopenia syndrome, an emerging tick-borne zoonosis. *Lancet Infect Dis* **14**, 763 – 772 (2014).

42. Kato, H. *et al.* Epidemiological and Clinical Features of Severe Fever with Thrombocytopenia Syndrome in Japan, 2013 – 2014. *PLoS ONE* **11**, e0165207 (2016).

43. Deng, B. *et al.* Clinical features and factors associated with severity and fatality among patients with severe fever with

thrombocytopenia syndrome Bunyavirus infection in Northeast China. *PLoS ONE* **8**, e80802 (2013).

44. Hu, J. *et al.* Correlations between clinical features and death in patients with severe fever with thrombocytopenia syndrome. *Medicine* **97**, e10848 (2018).

45. Ding, Y.-P. *et al.* Prognostic value of clinical and immunological markers in acute phase of SFTS virus infection. *Clin. Microbiol. Infect.* **20**, O870–8 (2014).

46. Shin, J., Kwon, D., Youn, S.-K. & Park, J.-H. Characteristics and Factors Associated with Death among Patients Hospitalized for Severe Fever with Thrombocytopenia Syndrome, South Korea, 2013. *Emerging Infect. Dis.* **21**, 1704–1710 (2015).

47. Li, H. *et al.* Epidemiological and clinical features of laboratory-diagnosed severe fever with thrombocytopenia syndrome in China, 2011–17: a prospective observational study. *Lancet Infect Dis* **18**, 1127–1137 (2018).

48. Sun, Y. *et al.* Early diagnosis of novel SFTS bunyavirus infection by quantitative real-time RT-PCR assay. *Journal of Clinical Virology* **53**, 48–53 (2012).

49. Yang, G. *et al.* Development and evaluation of a reverse transcription loop-mediated isothermal amplification assay for rapid detection of a new SFTS bunyavirus. *Arch Virol* **157**, 1779–1783 (2012).

50. Jiao, Y. *et al.* Preparation and Evaluation of Recombinant Severe Fever with Thrombocytopenia Syndrome Virus Nucleocapsid Protein for Detection of Total Antibodies in Human and Animal Sera by Double-Antigen Sandwich Enzyme-Linked Immunosorbent Assay. *J. Clin. Microbiol.* **50**, 372–377 (2012).

51. McCormick, J. B. *et al.* Lassa fever. Effective therapy with ribavirin. *N Engl J Med* **314**, 20–26 (1986).

52. Fisher-Hoch, S. P. *et al.* Crimean Congo-haemorrhagic fever treated with oral ribavirin. *Lancet* **346,** 472 – 475 (1995).

53. Huggins, J. W. *et al.* Prospective, double-blind, concurrent, placebo-controlled clinical trial of intravenous ribavirin therapy of hemorrhagic fever with renal syndrome. *J. Infect. Dis.* **164,** 1119 – 1127 (1991).

54. Lu, Q.-B. *et al.* Common adverse events associated with ribavirin therapy for Severe Fever with Thrombocytopenia Syndrome. *Antiviral Research* **119,** 19 – 22 (2015).

55. Cyranoski, D. East Asia braces for surge in deadly tick-borne virus. *Nature* **556,** 282 – 283 (2018).

56. Hofmann, H. *et al.* Severe fever with thrombocytopenia virus glycoproteins are targeted by neutralizing antibodies and can use DC-SIGN as a receptor for pH-dependent entry into human and animal cell lines. *Journal of Virology* **87,** 4384 – 4394 (2013).

57. Sun, Y. *et al.* Nonmuscle myosin heavy chain IIA is a critical factor contributing to the efficiency of early infection of severe fever with thrombocytopenia syndrome virus. *Journal of Virology* **88,** 237 – 248 (2014).

58. Plegge, T., Hofmann-Winkler, H., Spiegel, M. & Pöhlmann, S. Evidence that Processing of the Severe Fever with Thrombocytopenia Syndrome Virus Gn/Gc Polyprotein Is Critical for Viral Infectivity and Requires an Internal Gc Signal Peptide. *PLoS ONE* **11,** e0166013 (2016).

59. Dessau, M. & Modis, Y. Crystal structure of glycoprotein C from Rift Valley fever virus. *Proc. Natl. Acad. Sci. U.S.A.* **110,** 1696 – 1701 (2013).

60. Wu, Y. *et al.* Structures of phlebovirus glycoprotein Gn and identification of a neutralizing antibody epitope. *Proc. Natl. Acad. Sci. U.S.A.* **114,** E7564 – E7573 (2017).

61. Yu, L. *et al.* Critical Epitopes in the Nucleocapsid Protein of SFTS Virus Recognized by a Panel of SFTS Patients Derived Human Monoclonal Antibodies. *PLoS ONE* **7**, e38291 (2012).

62. Jin, J., Park, C., Cho, S.-H. & Chung, J. The level of decoy epitope in PCV2 vaccine affects the neutralizing activity of sera in the immunized animals. *Biochemical and Biophysical Research Communications* **496**, 846–851 (2018).

63. Shimada, S., Posadas-Herrera, G., Aoki, K., Morita, K. & Hayasaka, D. Therapeutic effect of post-exposure treatment with antiserum on severe fever with thrombocytopenia syndrome (SFTS) in a mouse model of SFTS virus infection. *Virology* **482**, 19–27 (2015).

64. Guo, X. *et al.* Human antibody neutralizes severe Fever with thrombocytopenia syndrome virus, an emerging hemorrhagic Fever virus. *Clin. Vaccine Immunol.* **20**, 1426–1432 (2013).

65. McCafferty, J., Griffiths, A. D., Winter, G. & Chiswell, D. J. Phage antibodies: filamentous phage displaying antibody variable domains. *Nature* **348**, 552–554 (1990).

66. Boder, E. T. & Wittrup, K. D. Yeast surface display for screening combinatorial polypeptide libraries. *Nature Biotechnology* **15**, 553–557 (1997).

67. Köhler, G. & Milstein, C. Continuous cultures of fused cells secreting antibody of predefined specificity. *Nature* **256**, 495–497 (1975).

68. Babcook, J. S., Leslie, K. B., Olsen, O. A., Salmon, R. A. & Schrader, J. W. A novel strategy for generating monoclonal antibodies from single, isolated lymphocytes producing antibodies of defined specificities. *PNAS* **93**, 7843–7848 (1996).

69. Tiller, T. *et al.* Efficient generation of monoclonal antibodies from single human B cells by single cell RT-PCR and expression

vector cloning. *Journal of Immunological Methods* **329**, 112–124 (2008).

70. Scheid, J. F. *et al.* Broad diversity of neutralizing antibodies isolated from memory B cells in HIV-infected individuals. *Nature* **458**, 636–640 (2009).

71. Reddy, S. T. *et al.* Monoclonal antibodies isolated without screening by analyzing the variable-gene repertoire of plasma cells. *Nature Biotechnology* **28**, 965–969 (2010).

72. Walker, L. M. & Burton, D. R. Passive immunotherapy of viral infections: 'super-antibodies' enter the fray. *Nat Rev Immunol* **18**, 297–308 (2018).

73. Salazar, G., Zhang, N., Fu, T.-M. & An, Z. Antibody therapies for the prevention and treatment of viral infections. *npj Vaccines 2017 2:1* **2**, 19 (2017).

74. Pascal, K. E. *et al.* Pre- and postexposure efficacy of fully human antibodies against Spike protein in a novel humanized mouse model of MERS-CoV infection. *PNAS* 201510830 (2015). doi:10.1073/pnas.1510830112

75. Flyak, A. I. *et al.* Cross-Reactive and Potent Neutralizing Antibody Responses in Human Survivors of Natural Ebolavirus Infection. *Cell* **164**, 392–405 (2016).

76. Stettler, K. *et al.* Specificity, cross-reactivity, and function of antibodies elicited by Zika virus infection. *Science* **353**, 823–826 (2016).

77. Wang, Q. *et al.* Molecular determinants of human neutralizing antibodies isolated from a patient infected with Zika virus. *Sci Transl Med* **8**, 369ra179–369ra179 (2016).

78. Walker, L. M. *et al.* Broad and potent neutralizing antibodies from an African donor reveal a new HIV-1 vaccine target. *Science* **326**, 285 – 289 (2009).

79. Wu, X. *et al.* Rational design of envelope identifies broadly neutralizing human monoclonal antibodies to HIV-1. *Science* **329**, 856 – 861 (2010).

80. BRUTON, O. C. Agammaglobulinemia. *Pediatrics* **9**, 722 – 728 (1952).

81. Stangel, M. & Pul, R. Basic principles of intravenous immunoglobulin (IVIg) treatment. *J. Neurol.* **253 Suppl 5**, V18 – 24 (2006).

82. Ferrara, G., Zumla, A. & Maeurer, M. Intravenous Immunoglobulin (IVIg) for Refractory and Difficult-to-treat Infections. *The American Journal of Medicine* **125**, 1036.e1 – 1036.e8 (2012).

83. Ishida, J. H. *et al.* Phase 1 Randomized, Double-Blind, Placebo-Controlled Study of RG7667, an Anticytomegalovirus Combination Monoclonal Antibody Therapy, in Healthy Adults. *Antimicrob. Agents Chemother.* **59**, 4919 – 4929 (2015).

84. Dole, K. *et al.* A First-in-Human Study To Assess the Safety and Pharmacokinetics of Monoclonal Antibodies against Human Cytomegalovirus in Healthy Volunteers. *Antimicrob. Agents Chemother.* **60**, 2881 – 2887 (2016).

85. Lim, J. J. *et al.* Two Phase 1, Randomized, Double-Blind, Placebo-Controlled, Single-Ascending-Dose Studies To Investigate the Safety, Tolerability, and Pharmacokinetics of an Anti-Influenza A Virus Monoclonal Antibody, MHAA4549A, in Healthy Volunteers. *Antimicrob. Agents Chemother.* **60**, 5437 – 5444 (2016).

86. Caskey, M. *et al.* Viraemia suppressed in HIV-1-infected humans by broadly neutralizing antibody 3BNC117. *Nature* **522**, 487–491 (2015).

87. Carbonell-Estrany, X. *et al.* Motavizumab for prophylaxis of respiratory syncytial virus in high-risk children: a noninferiority trial. *Pediatrics* **125**, e35–51 (2010).

88. Robbie, G. J. *et al.* A novel investigational Fc-modified humanized monoclonal antibody, motavizumab-YTE, has an extended half-life in healthy adults. *Antimicrob. Agents Chemother.* **57**, 6147–6153 (2013).

89. Park, S., Lee, D.-H., Park, J.-G., Lee, Y. T. & Chung, J. A sensitive enzyme immunoassay for measuring cotinine in passive smokers. *Clin. Chim. Acta* **411**, 1238–1242 (2010).

90. Lee, Y., Kim, H. & Chung, J. An antibody reactive to the Gly63|[ndash]|Lys68 epitope of NT-proBNP exhibits O-glycosylation-independent binding. *Experimental & Molecular Medicine* **46**, e114 (2014).

91. Andris-Widhopf, J., Steinberger, P., Fuller, R., RADER, C. & BARBAS, C. F., III. Generation of Human scFv Antibody Libraries: PCR Amplification and Assembly of Light- and Heavy-Chain Coding Sequences. *Cold Spring Harbor Protocols* **2011**, pdb.prot065573–pdb.prot065573 (2011).

92. BARBAS, C. F., III, Burton, D. R., Scott, J. K. & Silverman, G. J. Phage Display: A Laboratory Manual. *Cold Spring Harbor Laboratory Press* (2001). doi:10.1086/420571

93. Lee, S. *et al.* An antibody to the sixth Ig-like domain of VCAM-1 inhibits leukocyte transendothelial migration without affecting adhesion. *J. Immunol.* **189**, 4592–4601 (2012).

94. Kim, H.-Y., Tsai, S., Lo, S.-C., Wear, D. J. & Izadjoo, M. J. Production and Characterization of Chimeric Monoclonal

Antibodies against Burkholderia pseudomallei and B. mallei Using the DHFR Expression System. *PLoS ONE* **6**, e19867 (2011).

95. DULBECCO, R. & VOGT, M. Some problems of animal virology as studied by the plaque technique. *Cold Spring Harb. Symp. Quant. Biol.* **18**, 273–279 (1953).

96. Pimenova, T. *et al.* Epitope mapping on bovine prion protein using chemical cross-linking and mass spectrometry. *J Mass Spectrom* **43**, 185–195 (2008).

97. Corti, D. *et al.* Protective monotherapy against lethal Ebola virus infection by a potently neutralizing antibody. *Science* **371**, aad5224–1495 (2016).

98. Liu, Q. *et al.* Antibody-dependent-cellular-cytotoxicity-inducing antibodies significantly affect the post-exposure treatment of Ebola virus infection. *Sci Rep* **7**, 45552 (2017).

99. Gunn, B. M. *et al.* A Role for Fc Function in Therapeutic Monoclonal Antibody-Mediated Protection against Ebola Virus. *Cell Host & Microbe* **24**, 221–233.e5 (2018).

100. Pelegrin, M., Naranjo-Gomez, M. & Piechaczyk, M. Antiviral Monoclonal Antibodies: Can They Be More Than Simple Neutralizing Agents? *Trends in Microbiology* **23**, 653–665 (2015).

101. Casadevall, A., Dadachova, E. & Pirofski, L.-A. Passive antibody therapy for infectious diseases. *Nat Rev Micro* **2**, 695–703 (2004).

102. Bar, K. J. *et al.* Effect of HIV Antibody VRC01 on Viral Rebound after Treatment Interruption. *N Engl J Med* **375**, 2037–2050 (2016).

103. Scheid, J. F. *et al.* HIV-1 antibody 3BNC117 suppresses viral rebound in humans during treatment interruption. *Nature* **535**, 556–560 (2016).

104. Caskey, M. *et al.* Antibody 10-1074 suppresses viremia in HIV-1-infected individuals. *Nat Med* **23**, 185–191 (2017).

105. Zhu, Q. *et al.* A highly potent extended half-life antibody as a potential RSV vaccine surrogate for all infants. *Sci Transl Med* **9**, eaaj1928 (2017).

106. PREVAIL II Writing Group *et al.* A Randomized, Controlled Trial of ZMapp for Ebola Virus Infection. *N Engl J Med* **375**, 1448–1456 (2016).

107. Yu, F. *et al.* A Potent Germline-like Human Monoclonal Antibody Targets a pH-Sensitive Epitope on H7N9 Influenza Hemagglutinin. *Cell Host & Microbe* **22**, 471–483.e5 (2017).

108. Paules, C. I. *et al.* The Hemagglutinin A Stem Antibody MEDI8852 Prevents and Controls Disease and Limits Transmission of Pandemic Influenza Viruses. *J. Infect. Dis.* **216**, 356–365 (2017).

109. Ying, T. *et al.* Exceptionally potent neutralization of Middle East respiratory syndrome coronavirus by human monoclonal antibodies. *Journal of Virology* **88**, 7796–7805 (2014).

110. Corti, D. *et al.* Prophylactic and postexposure efficacy of a potent human monoclonal antibody against MERS coronavirus. *PNAS* **112**, 10473–10478 (2015).

111. Sapparapu, G. *et al.* Neutralizing human antibodies prevent Zika virus replication and fetal disease in mice. *Nature* **540**, 443–447 (2016).

112. Robbiani, D. F. *et al.* Recurrent Potent Human Neutralizing Antibodies to Zika Virus in Brazil and Mexico. *Cell* **169**, 597–609.e11 (2017).

113. Marston, H. D., Paules, C. I. & Fauci, A. S. Monoclonal Antibodies for Emerging Infectious Diseases – Borrowing from History. *N Engl J Med* **378**, 1469–1472 (2018).

114. Gowen, B. B. *et al.* Modeling Severe Fever with Thrombocytopenia Syndrome Virus Infection in Golden Syrian Hamsters: Importance of STAT2 in Preventing Disease and Effective Treatment with Favipiravir. *Journal of Virology* **91**, e01942–16 (2017).

115. Ikegami, T. *et al.* Distinct virulence of Rift Valley fever phlebovirus strains from different genetic lineages in a mouse model. *PLoS ONE* **12**, e0189250 (2017).

116. Weis, W. *et al.* Structure of the influenza virus haemagglutinin complexed with its receptor, sialic acid. *Nature* **333**, 426–431 (1988).

117. Tharakaraman, K., Subramanian, V., Cain, D., Sasisekharan, V. & Sasisekharan, R. Broadly Neutralizing Influenza Hemagglutinin Stem-Specific Antibody CR8020 Targets Residues that Are Prone to Escape due to Host Selection Pressure. *Cell Host & Microbe* **15**, 644–651 (2014).

118. Wu, Y. *et al.* A potent broad-spectrum protective human monoclonal antibody crosslinking two haemagglutinin monomers of influenza A virus. *Nat Comms* **6**, 7708 (2015).

119. Chai, N. *et al.* A broadly protective therapeutic antibody against influenza B virus with two mechanisms of action. *Nat Comms* **8**, 14234 (2017).

120. VanBlargan, L. A., Goo, L. & Pierson, T. C. Deconstructing the Antiviral Neutralizing-Antibody Response: Implications for

Vaccine Development and Immunity. *Microbiology and Molecular Biology Reviews* **80**, 989 – 1010 (2016).

121. Yoon, A. *et al.* An Anti–Influenza Virus Antibody Inhibits Viral Infection by Reducing Nucleus Entry of Influenza Nucleoprotein. *PLoS ONE* **10**, e0141312 (2015).

122. Halldorsson, S. *et al.* Shielding and activation of a viral membrane fusion protein. *Nat Comms* **9**, 349 (2018).

List of abbreviations

ALT. alanine aminotransferase

AST. aspartate aminotransferase

CDR. *complementary determining region*

CK-MB. creatine kinase myocardial b fraction

CPE. *cytopathic effects*

CPK. creatine phosphokinase

Cκ. *human immunoglobulin kappa constant region*

d.p.i.. *days post-infection*

DAPI. *4',6-diamidino-2-phenylindole dihydrochloride*

EBV. *Epstein-Barr Virus*

ELISA. *enzyme-linked immunosorbent assay*

Fc. Fragment crystallizable

FFU. *focus forming unit*

FITC. *fluorescein isothiocyanate*

FRNT. *focus reduction neutralization test*

HA. *influenza hemagglutinin*

HCDR. *heavy chain complementary determining region*

HEK. *human embryonic kidney*

HIV. *Human Immunodeficiency Virus*

HRP. *horseradish peroxidase*

ICTV. *International Committee on Taxonomy of Viruses*

IFA. *immunofluorescence assay*

IFNAR1. *type I interferon (interferon α/β) receptor gene*

Ig. *immunoglobulin*

IGHG1. *human immunoglobulin heavy constant gamma1*

IMGT. *International Immunogenetics Information System*

K_D. *equilibrium dissociation constant*

k_{off}. *dissociation rate*

k_{on}. *association rate*

LDH. lactate dehydrogenase

MALDI. *mass matrix-assisted laser desorption/ionization*

MOF. multi organ failure

PBS. *phosphate buffered saline*

PFU. *plaque forming unit*

RPMI. *Roswell Park Memorial Institute*

RSV. *Respiratory Syncytial Virus*

RVFV. Rift Valley fever virus

s.d.. *standard deviations*

scFv. *single-chain variable fragment*

SFTS. *Severe Fever with Thrombocytopenia Syndrome*

SFTSV. *SFTS Virus*

$TCID_{50}$. *fifty-percent tissue culture infective dose*

TMB. *3,3′,5,5′-tetramethylbenzidine*

TOF. *time of flight*

ViPR. *Virus Pathogen Database and Analysis Resource*

요약(국문초록)

중증열성혈소판감소증후군은 최근 생겨난 감염병으로, 중국, 일본, 한국 지역에 제한적으로 발생하며, 심한 체내 출혈과 높은 치사율을 보인다. 현재 이 바이러스 질환에 대한 특이적인 백신이나 치료제가 허가된 바는 없다.

중증열성혈소판감소증후군의 치료제를 개발하기 위해, 먼저 중증열소판감소증후군 바이러스의 감염에서 회복한 환자로부터 수립된 파지-항체 라이브러리로부터 항체들을 분리해냈다.

그 중, Ab10 으로 명명한 항체는 중증열성혈소판감소증후군 바이러스의 Gn 외막 당단백질에 반응하였고, 시험관내 세포실험과 동물실험에서 숙주 세포와 A129 마우스의 중증열성혈소판감소증후군 바이러스 감염을 막는 효과를 보였다. 특히, Ab10 항체의 보호 효과는 치사량의 바이러스가 주입된 5 일 이후에도 80%의 마우스에서 보여졌다.

가교제를 이용한 질량분석과 알라닌 아미노산 치환 스캔 기법을 통해 Gn 당단백질의 도메인 2 과 줄기 부분에 존재하는 Ab10 항체의 구조적 결합 부위 위치를 찾아낼 수 있었고, 이는 Ab10 항체가 바이러스와 숙주 세포간 세포막 결합에 중요한 바이러스의 구조 변화를 막을 수 있음을 보여준다.

Ab10 항체는 Gangwon/Korea/2012, HB29, SD4 바이러스 변종의 재조합 Gn 당단백질에 모두 결합했다. 그리고 항체 결합 부위를 토대로 하여 분석한 결과, 기존에 발표된 272 종의 중증열성혈소판감소증후군 바이러스 분리주들 중 247 종에서 Gn 당단백질에 결합할 수 있다고 예측되었다.

따라서, 이들 결과는 Ab10 항체가 치료제로서 개발될 가능성이 높으며, 90% 이상의 중증열성혈소판감소증후군 바이러스 분리주들로 부터 보호 효과를 보일 수 있음을 시사한다.

중심어: 신종 바이러스, 중증열성혈소판감소증후군 바이러스, 바이러스 중화 항체, 단일클론 항체 치료제

학번: 2015-30613